

# The Chemical Properties of Milky Way and M31 Globular Clusters: II. Stellar Population Model Predictions

Michael A. Beasley

*Lick Observatory, University of California, Santa Cruz, CA 95064, USA*

mbeasley@ucolick.org

Jean P. Brodie

*Lick Observatory, University of California, Santa Cruz, CA 95064, USA*

brodie@ucolick.org

Jay Strader

*Lick Observatory, University of California, Santa Cruz, CA 95064, USA*

strader@ucolick.org

Duncan A. Forbes

*Centre for Astrophysics & Supercomputing, Swinburne University, Hawthorn, VIC 3122, Australia*

dforbes@astro.swin.edu.au

Robert N. Proctor

*Centre for Astrophysics & Supercomputing, Swinburne University, Hawthorn, VIC 3122, Australia*

rproctor@astro.swin.edu.au

Pauline Barmby

*Harvard-Smithsonian Center for Astrophysics, 60 Garden Street, Cambridge, MA 02138, USA*

pbarmby@cfa.harvard.edu

John P. Huchra

*Harvard-Smithsonian Center for Astrophysics, 60 Garden Street, Cambridge, MA 02138, USA*

huchra@cfa.harvard.edu

**ABSTRACT**

We derive ages, metallicities and abundance ratios ( $[\alpha/\text{Fe}]$ ) from the integrated spectra of 23 globular clusters in M31, by employing multivariate fits to two different stellar population models. We also perform a parallel analysis on 21 Galactic globular clusters as a consistency check, and in order to facilitate a differential analysis. Our analysis shows that the M31 globular clusters separate into three distinct components in age and metallicity; we identify an old, metal-poor group (7 clusters), an old, metal-rich group (10 clusters) and an intermediate age (3–6 Gyr), intermediate-metallicity ( $[Z/H]\sim-1$ ) group (6 clusters). This third group is not identified in the Galactic globular cluster sample. The majority of globular clusters in both samples appear to be enhanced in  $\alpha$ -elements, but the degree of enhancement is rather model-dependent. The intermediate age GCs appear to be the most enhanced, with  $[\alpha/\text{Fe}]\sim 0.4$ . These clusters are clearly depressed in CN with respect to the models and the bulk of the M31 and Milky Way sample. Compared to the bulge of M31, M32 and NGC 205, these clusters most resemble the stellar populations in NGC 205 in terms of age, metallicity and CN abundance. We infer horizontal branch morphologies for the M31 clusters using the Rose (1984) Ca II index, and demonstrate that blue horizontal branches are not leading to erroneous age estimates in our analysis. We discuss and reject as unlikely the hypothesis that these objects are in fact foreground stars contaminating the optical catalogs. The intermediate age clusters have generally higher velocities than the bulk of the M31 cluster population. Spatially, three of these clusters are projected onto the bulge region, the remaining three are distributed at large radii. We discuss these objects within the context of the build-up of the M31 halo, and suggest that these clusters possibly originated in a gas-rich dwarf galaxy, which may or may not be presently observable in M31.

*Subject headings:* globular clusters: general – galaxies: individual: M31

## 1. Introduction

Hubble (1932) was the first to identify and study globular clusters in the Andromeda galaxy (M31). From photographic plates obtained using the 100-inch telescope at Mount Wilson, he identified 140 objects apparently associated with M31 for which he stated “...*from their forms, structure, colors, luminosities and dimensions they are provisionally identified as globular clusters.*”. From the spectrum of “object No. 62”, he derived a radial velocity of  $-210\pm 100$   $\text{kms}^{-1}$ , consistent with the radial velocity of M31, thereby reinforcing the notion that these were clusters associated with the galaxy, and not seen in projection (nor indeed, were they background galaxies).

Despite their importance, and decades of study since Hubble, our knowledge about the chemical properties and ages of globular clusters (GCs) in M31 is limited. Fine abundance analysis, the primary method for determining the chemical compositions of stars, is currently beyond the

capabilities of current instrumentation for M31 GCs. Color-magnitude diagrams below the turn-off, the most reliable method for age determinations of stellar populations, are extremely challenging for current instrumentation, and at the distance of M31 suffer from the dual effects of crowding and the intrinsic faintness of cluster stars (e.g., Rich et al. 1996; Stephens et al. 2001)<sup>1</sup>. Thus, the determination of fundamental parameters such as metallicity have relied upon studies of their integrated light (e.g., van den Bergh 1969; Burstein et al 1984; Battistini et al. 1987; Tripicco 1989; Huchra et al. 1991; Jablonka et al. 1992; Jablonka et al. 1998; Ponder et al. 1998; Barmby et al. 2000; Perrett et al. 2002; Jiang et al. 2003.)

The general picture which has emerged from studies such as these is that M31’s GCs are broadly similar to their counterparts in the Milky Way. Both the Milky Way and M31 GC system metallicity ( $[\text{Fe}/\text{H}]$ )<sup>2</sup> distributions are consistent with being bimodal, with peaks at  $[\text{Fe}/\text{H}] \sim -1.5$  and  $\sim -0.5$  (Huchra et al. 1991; Barmby et al 2000; Perrett 2004). The most notable difference in terms of the chemical properties of the two cluster systems is that CN in the M31 clusters appears to be significantly enhanced with respect to Milky Way GCs (Burstein et al. 1984; Brodie & Huchra 1991; Tripicco 1989; Beasley et al. 2004; henceforth Paper I). On the basis of stellar modelling (Tripicco & Bell 1992) and observations of the near-UV NH feature (Ponder et al 1998; Li & Burstein 2003), the interpretation is that N is significantly enhanced in the M31 GCs.

The majority of GCs in M31 appear to be old, although there have been claims for the existence of a few intermediate age clusters (Jablonka et al. 1998; Jiang et al. 2003; Trager 2004). Based upon optical and near-IR colors, Barmby & Huchra (2000) have claimed that the ensemble of metal-rich GCs in M31 may be up to 4 Gyr younger than their metal-poor counterparts. In Paper I we showed that a number of star clusters in M31, identified as having thin-disk like kinematics (Morrison et al. 2004) are young objects ( $< 1$  Gyr old) with near-solar metallicities. We refer to these objects as ‘star clusters’ rather than GCs since, in the absence of spectroscopic mass estimates for these clusters, it is presently unclear whether they possess true globular cluster masses (e.g., Larsen et al. 2004), or are more akin to open clusters<sup>3</sup>.

Notwithstanding, the majority of these studies, in particular the spectroscopic ones, have by necessity been rather qualitative in nature, since only recently have stellar population models been available which can account for a range of metallicities, ages and  $\alpha$ -element abundance ratios (see Trager et al. 2000; Proctor & Sansom 2002; Thomas, Maraston & Bender 2003; Proctor, Forbes & Beasley 2004; hereafter PFB04). In this paper, we compare the Galactic and M31 GC samples presented in Paper I with contemporary stellar population models to estimate their ages,

---

<sup>1</sup>In an heroic effort, Brown et al. (2004) have recently published a CMD to the turn-off for an M31 GC. They derive an age of  $\sim 10$  Gyr for GC 312-035.

<sup>2</sup>Unless otherwise stated,  $[\text{Fe}/\text{H}]$  refers to metallicities on the Zinn & West (1984) scale.  $[\text{Z}/\text{H}]$  refers to ‘total’ metallicity, and  $[\alpha/\text{Fe}]$  represents the logarithmic ratio of  $\alpha$ -capture elements (e.g., O, Mg, Ca...) to iron.

<sup>3</sup>This terminology for star clusters may be a semantic point. However, it is important to recognize that no star clusters of globular cluster mass  $\gtrsim 10^4 M_\odot$  are thought to be associated with the Galactic thin disk.

metallicities, and  $[\alpha/\text{Fe}]$  ratios.

This paper is organized in the following fashion. In Section 2 we briefly summarize the data used in this study. In Section 3 we discuss the models and their correction for non-solar abundance ratios. In Section 4, we discuss our methodology and derive fundamental parameters (age, metallicity,  $[\alpha/\text{Fe}]$ ) for the Milky Way and M31 GCs. The physical nature of six intermediate age cluster candidates in M31 are discussed in Section 4.4. Section 5 presents an estimation of the horizontal branch morphologies of the M31 GCs based upon integrated spectra. Finally, in Section 6, we discuss the results of this study.

## 2. Galactic and M31 Data

The Milky Way and M31 GC data used here were discussed in detail in Paper I. To summarize, we use 20 high-quality integrated spectra for Milky Way globular clusters taken from Puzia et al. (2002; hereafter P02) and Cohen, Blakeslee & Ryzhov (1998; hereafter CBR98). The M31 data were first discussed in Barmby et al. (2000), and were re-analysed following procedures given in Paper I. Here we analyze 23 M31 GCs, excluding the young disk objects identified in Paper I. Unless otherwise stated, the P02 and CBR98+M31 data have been corrected onto the Lick spectroscopic system using the offsets given in P02 and Paper I respectively. All the Lick indices used here employ the Trager et al. (1998) definitions (supplemented by the higher order Balmer lines given by Worthey & Ottaviani 1997), which provide greater consistency with the Worthey (1994) fitting functions than the definitions given in Worthey et al. (1994) (G. Worthey, private comm.). These data have been augmented by an integrated spectrum of the outer bulge of the Milky Way (P02) and integrated spectra for the central bulge of M31 ( $r_e/8$  aperture), and two of its companions M32 (NGC 221) and NGC 205 (Trager et al. 1998).

## 3. Stellar Population Models for Non-solar Abundance Ratios

It has been known for some time that elliptical galaxies (and Milky Way GCs) exhibit  $[\alpha/\text{Fe}]$  ratios which differ from the local abundance pattern (e.g. Worthey, Faber & González 1992). In order to quantify the metallicities and ages of such systems, various attempts have been made to either empirically or theoretically calibrate models which account for non-solar abundance patterns (e.g. Barbuy 1994; Borges et al. 1995; Milone et al. 2000). However, only recently have comprehensive models been available which can account for a wide range of metallicity, age and  $\alpha$ -element abundances in the commonly used Lick system (Trager et al. 2000; Proctor & Sansom 2002; Thomas, Maraston & Bender 2003; Tantalo et al. 2004).

In this paper, we considered three different single stellar population (SSP) models, those of Vazdekis (1999; henceforth V99), Bruzual & Charlot (2003; henceforth BC03) and those of Thomas, Maraston & Bender (2003; henceforth TMB03). The V99, BC03 and TMB03 models

provide indices based on Lick fitting functions, which define relations between index strength and metallicity, effective temperature and gravity. In addition, V99 and BC03 make available spectral energy distributions which allow flexibility in defining and measuring line-strength indices. Here we have used indices based upon the fitting-functions to retain greater consistency among the models.

The V99 and BC03 models do not take into account non-solar abundance ratios, and we have attempted to do so using the method described in Trager et al. (2000). Note that we use the Trager et al. (2000) method, which assumes a fixed  $[Z/H]$ , rather than that discussed by Proctor & Sansom (2002), which assumes a fixed  $[Fe/H]$ , since the former is more appropriate for metal-poor stellar populations (Proctor & Sansom 2002). Briefly, the corrections referred to above require a knowledge of the following: *(i)* the abundance ratio pattern of the stars in the SSP model stellar library, *(ii)* the difference between this pattern and objects in question (in this case GCs), *(iii)* the impact of this difference on the model isochrones used to construct the SSP and *(iv)* the change in line-strength indices due to a given change in the abundance ratio pattern for a given isochrone (synthetic 'response' functions). There are a number of caveats and limitations to these corrections; e.g., point *(i)* has yet to be homogeneously characterised for any stellar library, whilst the Tripicco & Bell (1995) response functions required in point *(iv)* were only performed for a very limited parameter space (three stars), with what are now rather old atomic linelists. For a full discussion of the treatment of varying abundance ratios in the models, see Trager et al. (2000), Proctor & Sansom (2002), Proctor et al. (2004) and PFB04.

The TMB03 models already account for variations in  $[\alpha/Fe]$ , and now include corrections for the higher-order Balmer lines (Thomas, Maraston & Korn 2004; henceforth TMK04) which were not modeled by Tripicco & Bell (1995). For all three models, we find reasonable consistency between their age, metallicity and  $[\alpha/Fe]$  predictions for the GC data (see PFB04 and Section 4.2). For this reason, and due to the fact that the V99 models do not extend to metallicities below  $[Fe/H]=-1.7$ , we only utilise the BC03 and TMB03+TMK04 models (these latter two models referred to collectively as TMB03) in what follows.

#### 4. Analysis

In order to characterize where the M31 and Milky Way GCs lie in the parameter space of the models, we begin by examining the behaviour of some individual indices. In Section 4.2, we perform more quantitative multivariate fits to identify which modeled combinations of age, metallicity and  $[\alpha/Fe]$  best describe these data. To preview some of the results of our age-metallicity analysis, six M31 GCs (including 292-0101, an intermediate age cluster identified in Paper I) appear to be of intermediate age ( $\sim 5$  Gyr) and have intermediate metallicities ( $[Z/H]\sim-1.0$ ). These GCs are indicated as such in the following Section, and the justification for this is given in Section 4.2.

#### 4.1. Index-Index Comparisons

In Figure 1 we plot  $\langle \text{Fe} \rangle^4$  versus Mg  $b$  for the M31 and Milky Way GCs, compared to the TMB03 models. This combination of indices has been shown to possess differing sensitivities to Fe-peak and  $\alpha$ -element abundance ratios (Tripicco & Bell 1995), and can therefore be used to track the variation of  $[\alpha/\text{Fe}]$  (Trager et al. 2000; TMB03). As already demonstrated by TMB03, and can be seen in Figure 1, the Milky Way data occupy a position at approximately  $[\alpha/\text{Fe}] = +0.3$ , which is roughly consistent with high-dispersion estimates for Milky Way GCs (e.g., see the compilation of Carney 1996; Gratton et al. 2004). Based on this figure, the M31 GCs also appear to be enhanced in  $\alpha$ -elements, but at the level of  $[\alpha/\text{Fe}] = +0.2$  for Mg  $b > 1.5$ , slightly less than that seen in the Milky Way clusters (see also Kuntschner et al. 2002 and Trager 2004). At Mg  $b < 1.5$ , the TMB03 models suggest  $[\alpha/\text{Fe}] \leq 0$ , behavior which is also hinted at for the CBR98 data but not for that of P03. Whether this is a failure of the models, or a calibration problem in the M31 and CBR98 data is unclear at present.

Assuming that the M31 clusters have comparable ages to their Galactic counterparts (an as yet untested assumption), then based on Figure 1 we may conclude that the M31 GCs are  $\alpha$ -enhanced in a broadly similar fashion to that seen in Milky Way GCs and massive elliptical galaxies (e.g. Carney 1996; Trager et al. 2000)<sup>5</sup>. The bulges of both the Milky Way and M31 also appear to be  $\alpha$ -enhanced at the 0.2 dex level, based on Figure 1, consistent with previous findings (e.g., McWilliam & Rich 1994 and Trager et al. 2000 respectively). The position of the compact elliptical M32, suggests that this galaxy has  $[\alpha/\text{Fe}]$  ratios closer to the solar value, whereas that of the dE NGC 205 suggests  $[\alpha/\text{Fe}] < 0.0$ .

---

<sup>4</sup> $(\text{Fe}5270 + \text{Fe}5335)/2$

<sup>5</sup>We note that de Freitas Pacheco (1997) concluded that the 12 M31 GCs from Burstein et al. (1984) exhibited  $[\text{Mg}/\text{Fe}] = 0.35 \pm 0.10$ , which is consistent with our findings. Unfortunately, this study does not go into sufficient detail to allow a comprehensive appraisal.

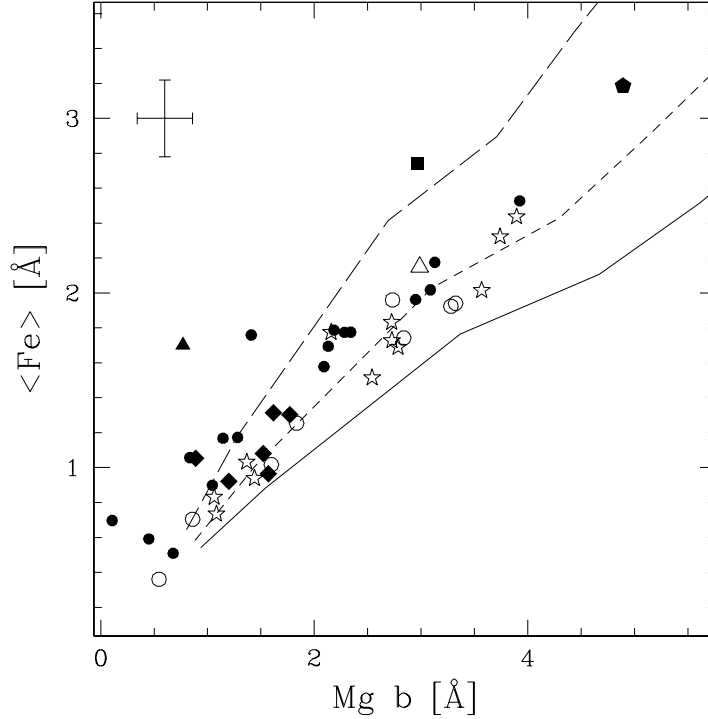


Fig. 1.— Predictions of the Thomas, Maraston & Bender (2003) stellar population models for various  $[\alpha/\text{Fe}]$  ratios versus the Milky Way and M31 GC data. Solid circles represent M31 GCs, open symbols Milky Way GCs (stars:P02; circles:CBR98). Models are for 12 Gyr stellar populations, with  $[\alpha/\text{Fe}] = 0.5, 0.3$  and  $0.0$  (solid, short-dashed and long-dashed lines respectively). Also shown are the Milky Way bulge data from P02 (open triangle), and data for the M31 bulge, M32 and NGC 205 from Trager et al. (1998) (filled pentagon, square and triangle respectively). The median error of the M31 sample is shown in the top-left of the figure. The large diamonds are M31 clusters which we identify as intermediate age.

For several combinations of indices such as those displayed in Figure 1, consistent results are obtained for the GC  $[\alpha/\text{Fe}]$  ratios. This is true for some combinations of Lick ‘iron’ indices (e.g., Fe4383, Fe5270, Fe5335, Fe5709), and ‘magnesium’ indices ( $\text{Mg}_2$  &  $\text{Mg } b$ ). However, for a number of indices the models do not well describe the behaviour of the Galactic GC data (TMB03), and this is also true of the M31 GCs. It is not immediately clear why the index combination in Figure 1 should be preferred over other permutations of indices, other than its ability to fit the Galactic GC data. This is one reason why we prefer the multivariate approach described in Section 4.2.

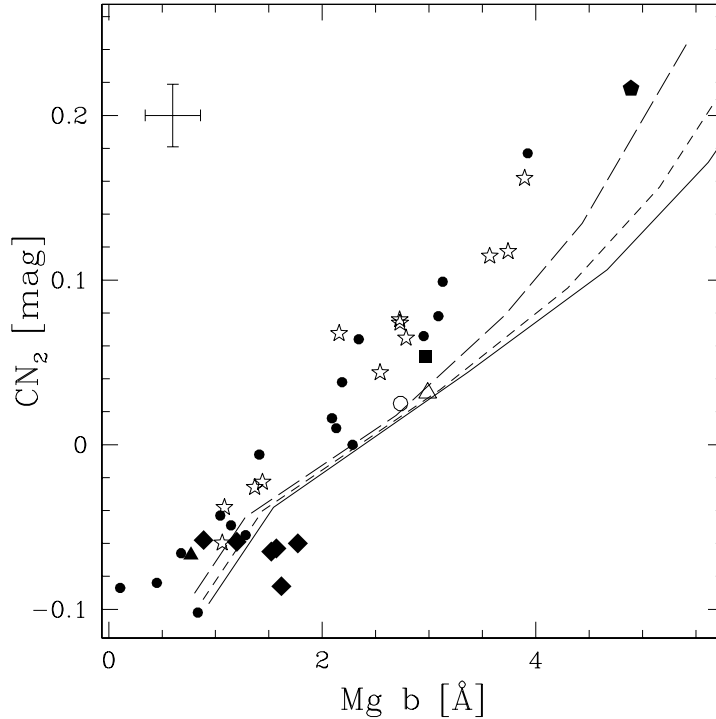


Fig. 2.— Mg  $b$  and CN<sub>2</sub> indices for the M31 and Milky Way GCs, plotted with the predictions of the Thomas, Maraston & Bender (2003) stellar population models. Models are for 12 Gyr stellar populations, with  $[\alpha/\text{Fe}] = 0.5, 0.3$  and  $0.0$  (solid, short-dashed and long-dashed lines respectively). Symbols are as for the previous figure, but note that the CBR98 data are not included since they do not extend to CN<sub>2</sub>. The CN<sub>2</sub> indices of the GCs and M31 bulge are clearly too strong for the models. The M31 GCs identified as intermediate age (diamonds) appear *depressed* in CN<sub>2</sub> with respect to the models and bulk of M31 and Milky Way clusters.

Three of the discrepant indices include the Lick CN indices and Ca4227, which are affected by variations in N and C (e.g., Tripicco & Bell 1995; Vazdekis et al. 1997; Schiavon et al. 2002). By way of illustration, we show the Lick CN<sub>2</sub> band versus Mg  $b$  in Figure 2. The CN<sub>2</sub> (and the CN<sub>1</sub> band - not shown) is generally too strong compared to the models for both the Milky Way clusters (see TMB03) and M31. The existence of strong CN enhancement in M31 GCs when compared to the local abundance pattern, interpreted as N enhancement, has been known for some time (Burstein et al. 1984; Brodie & Huchra 1991; Ponder et al. 1998; Li & Burstein 2003; Burstein et al. 2004). The M31 GCs in Figure 2 do not appear enhanced in CN compared to the Milky Way clusters, although note that the Lick correction for the M31 data is rather uncertain and large ( $\sim 0.03$  mag, see Paper I). However, the near-UV cyanogen feature at  $\lambda 3883$  does appear enhanced in M31 clusters when compared to their Galactic counterparts (Paper I), possibly suggesting flux-calibration problems with the Lick CN index. The bulge of M31 also appears to be quite CN-strong,



which is not the case for (the more metal-poor) Galactic bulge. TMB03 found that they could fit the CN indices of the Milky Way data by assuming  $[\alpha/N]=-0.5$ , or in other words by increasing N by a factor of 3 with respect to the  $\alpha$ -elements. Presumably, the M31 GCs are enhanced in N by at least a similar factor.

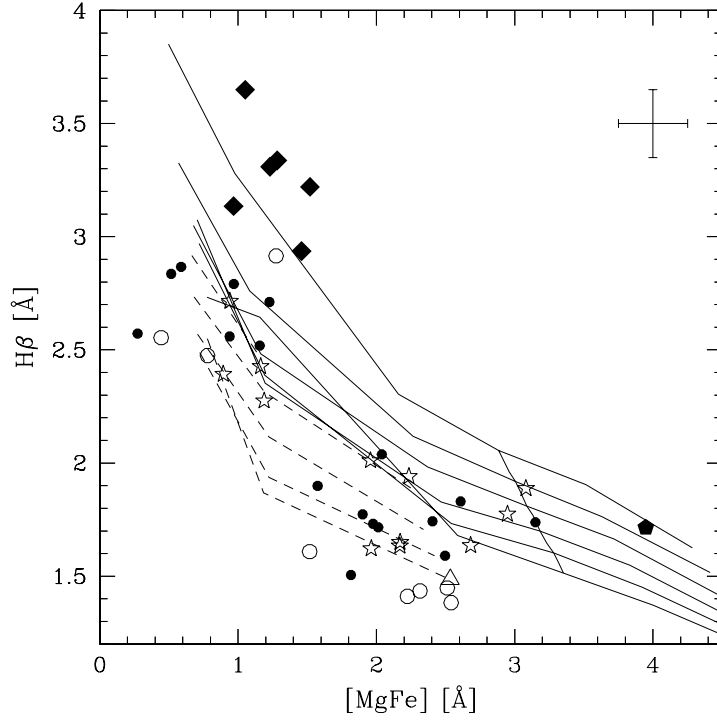


Fig. 3.— The  $H\beta$  indices as a function of  $[MgFe]$  for the M31 (filled circles) and Milky Way GCs (open circles: CBR98; open stars: P02). Overplotted are the Thomas, Maraston & Korn (2004) models assuming  $[\alpha/Fe]=+0.3$  for ages 5,7,9,11,13 & 15 Gyr (solid lines). The single angled line at  $[MgFe]\sim 3$  represent an isometallicity line of  $[Z/H]=0.0$ . The dashed lines represent the models of Maraston & Thomas (2000) for ages 9,11,13 & 15 Gyr at  $[Z/H]\leq -0.5$ , which assume no mass-loss on the red giant branch (see text). Six M31 clusters (diamonds) have clearly enhanced  $H\beta$ .

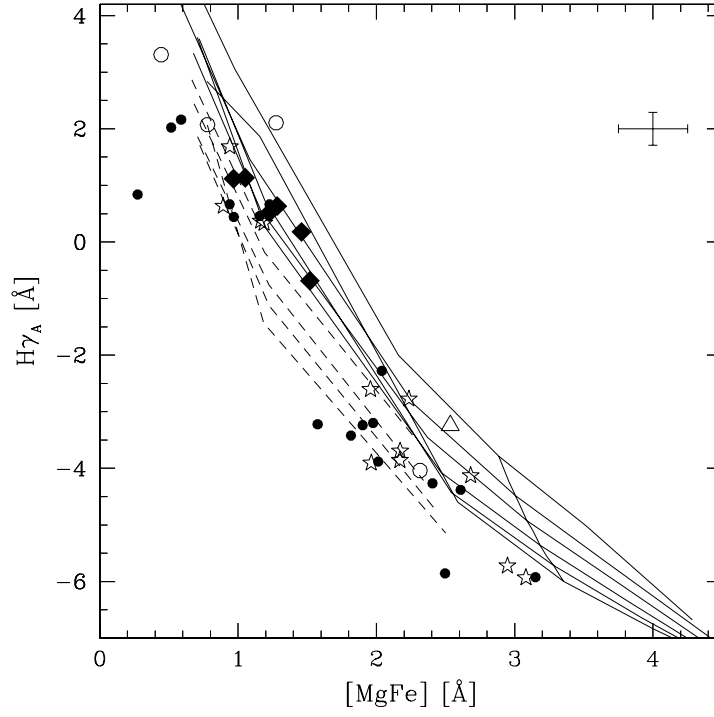


Fig. 4.— The  $H\gamma_A$  indices as a function of  $[MgFe]$ . Symbols as for previous figure.

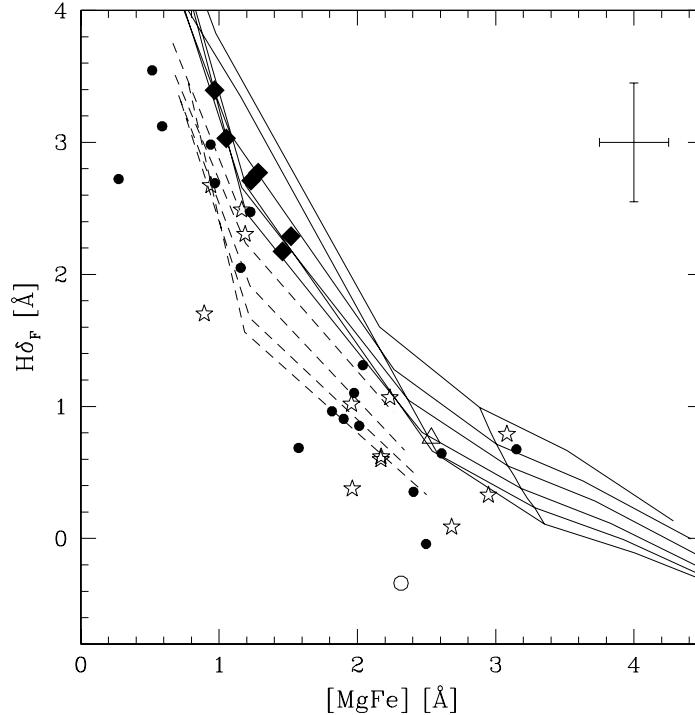


Fig. 5.— The  $H\delta_F$  indices as a function of  $[MgFe]$ . Symbols as for Figure 3.

The positions of the Milky Way and M31 GCs in the  $H\beta$ – $[MgFe]$  planes of the TMK04 models are shown in Figure 3. Here, we have adopted the  $[\alpha/Fe]=+0.3$  models of TMK04, consistent with the location of these data in Figure 1. These data span a wide range of metallicities, approximately  $-2.0 \leq [Z/H] \leq 0$ . Figures 4 and 5 show these data in the  $H\gamma_A$ – $[MgFe]$  and  $H\delta_F$ – $[MgFe]$  planes respectively. Both the Milky Way and M31 GCs generally define similar, old-age sequences in  $H\beta$ ,  $H\gamma_A$  and  $H\delta_F$  (we have not used  $H\gamma_A$  since this index showed large calibration uncertainties in the M31 data; see Paper I). Many of the data points fall off the bottom of the TMK04 grids, suggesting that only lower limits may be derived for many clusters from these diagrams. The dashed lines indicate the models of Maraston & Thomas (2000), which assume generally red horizontal branches, and have not been corrected for the local  $[\alpha/Fe]$  abundance pattern<sup>6</sup>. These model variants do a much better job of following the data, suggesting rather modest mass-loss on the red giant branch (hence, redder horizontal branches) for stars in these clusters.

We identify five M31 clusters (126-184, 301-022, 337-068, NB16, and NB67) as intermediate age and of intermediate metallicity. They appear particularly anomalous in the  $H\beta$ – $[MgFe]$  plot,

---

<sup>6</sup>At low metallicities, these models actually reflect an  $\alpha$ -enhanced pattern following Galactic halo stars (TMB03).

but appear more ‘normal’ in their higher-order Balmer lines. Closer inspection of Figures 4 and 5 suggest that these objects also define a different locus in  $H\gamma_A$  and  $H\delta_F$ . These objects lie in a region very similar to the metal-poor, old GCs and without the benefit of SSP models were not identified as being particularly unusual in Paper I.

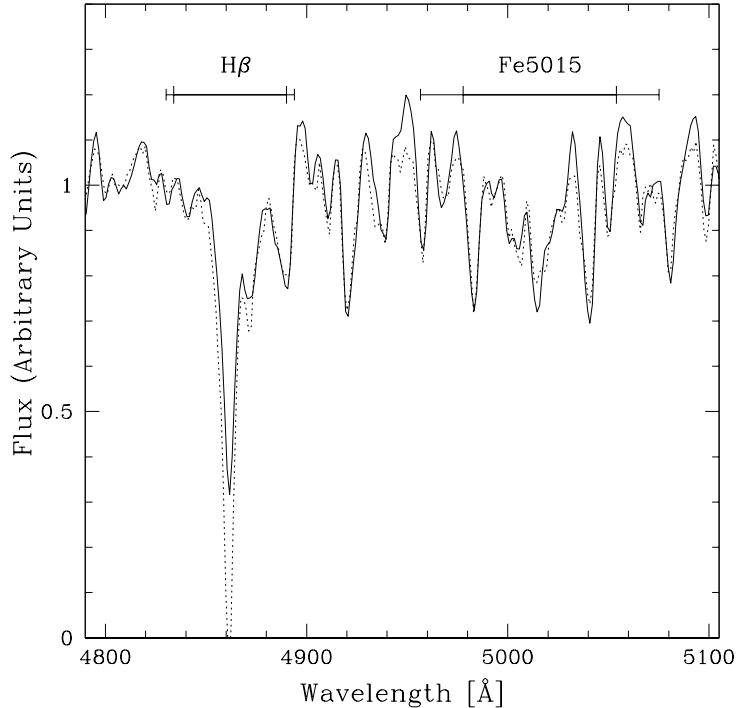


Fig. 6.— A comparison of the spectra of two GCs, 158-213 and 337-068 in M31, which have similar metallicities but different ages. The spectra are shown in a narrow wavelength range to illustrate important similarities and differences between the two spectra. The index and continuum passbands of the Lick  $H\beta$  and Fe5015 indices are marked. The solid line indicates the spectrum of 158-213, an old GC ( $12.1 \pm 0.9$  Gyr) with  $[Z/H] = -0.8 \pm 0.2$  (Thomas, Maraston & Bender 2003 models). The dotted line shows 337-068, an IAGC ( $6.6 \pm 3.2$  Gyr) with  $[Z/H] = -1.0 \pm 0.2$ . Note the fairly good agreement between the metallicity-sensitive Fe5015 index, but the significantly stronger  $H\beta$  absorption in the younger GC.

To illustrate the differences in the  $H\beta$  indices between the intermediate age and old GCs, a comparison of the spectra of the M31 GCs 158-213 and 337-068 is shown in Figure 6. These clusters are at roughly similar metallicities ( $[Z/H] \sim -1.0$ ), but cluster 337-068, which we identify as being intermediate age, has significantly stronger  $H\beta$  absorption. The similar metallicities of these clusters is confirmed by comparison of the Fe5015 index (the slightly weaker Fe5015 index in 337-068 with respect to 158-213 can be explained purely by the age, rather than metallicity difference between these clusters). Strong Balmer-lines in M31 GCs have been noted previously (Spinrad & Schweizer 1972; Rabin 1981; Burstein et al. 1984) and are not in themselves sufficient

evidence for young ages. Stellar populations such as hot horizontal branch stars can also contribute to absorption in the Balmer lines. In the next section we justify our identification of intermediate ages for these clusters.

## 4.2. Model Comparisons through Multivariate Fitting

Based upon diagnostic plots of individual indices such as shown in Figure 3, age, metallicity and abundance ratio determinations of the GCs in our sample are often ambiguous. The combination of observational errors (systematic+random), and modeling uncertainties in the Balmer lines (e.g., due to horizontal branch morphology variations) make age estimations particularly uncertain. This is well illustrated in Figures 3, 4 and 5 for the most metal-rich Galactic GC in this study, NGC 6553 (from P02). The  $H\beta$  index predicts an age of  $\sim 7$  Gyr for this cluster,  $H\gamma_A$  predicts ages  $\geq 15$  Gyr, while  $H\delta_F$  yields  $\sim 6$  Gyr. Although in the absence of a preference of one index over another, a weighted mean age may be appropriate, this is an appreciable age-range for what is thought to be a  $\sim 13$  Gyr cluster from its CMD (Zoccali et al. 2001).

Therefore, we have opted to use the method outlined in PFB04, and utilized in Paper I<sup>7</sup> and Pierce et al. (2004, MN submitted). PFB04 implement a straightforward  $\chi^2$  minimization technique between measured Lick indices and SSP models, in order to identify the best model solution for age, metallicity and  $[\alpha/Fe]$ . This method, in somewhat different forms, has been successfully used for galaxies (e.g., Vazdekis et al. 1997; Proctor & Sansom 2002) and GCs (e.g., de Freitas Pacheco 1997, – see also Barmby & Huchra 2000). In essence, the entire suite of measured Lick indices are compared to the full grid of model indices, which are searched for the best solution for the above parameters. Any indices which significantly deviate (by  $> 3 \sigma$ ) are clipped from the fit and  $\chi^2$  re-calculated. This procedure is iterated until no further indices are removed and a stable solution obtained. As demonstrated by PFB04, the method is robust, and recovers reliable ages, metallicities and abundance ratios for Galactic GCs using the V99, BC03 and TMB03 models.

---

<sup>7</sup>We have elected not to list derived  $[\alpha/Fe]$  ratios for the young disk clusters identified in Paper I, since the model predictions are highly uncertain at such young ages. However, we note that the  $Mg\ b/(Fe)$  ratios of these objects are consistent with solar-scaled  $[\alpha/Fe]$  ratios.

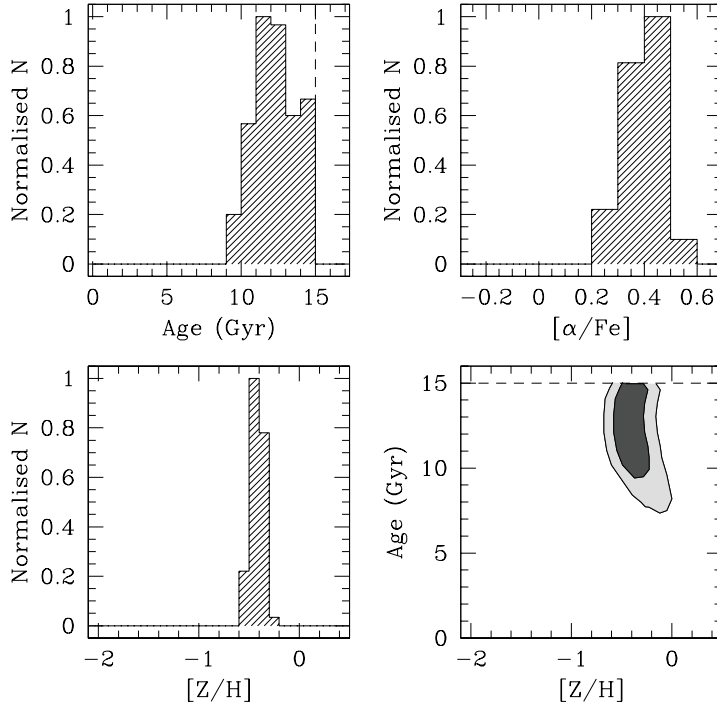


Fig. 7.— The  $1\text{-}\sigma$  confidence distributions for age, metallicity and  $[\alpha/\text{Fe}]$  for NGC 6536, after performing a  $\chi^2$  fit to the Thomas, Maraston & Bender (2003) SSP models. The bottom-right panel shows the  $1\text{-}\sigma$  and  $2\text{-}\sigma$  confidence regions in the  $[\text{Z}/\text{H}]$ –Age plane. The banana-shape of this region illustrates that age and metallicity are still degenerate in the solution. The dashed lines in the top-left and bottom-right panels indicate the upper age-limit (15 Gyr) in the models. The piling up in the oldest bin in the top-left panel is artificial.

An example of the application of this method to the moderately metal-rich Galactic GC NGC 6536 (P02 data) is shown in Figure 7. The best-fit parameters for this GC, based upon the TMB03 (BC03) models, are  $[\text{Z}/\text{H}] = -0.4 \pm 0.1$  ( $-0.7 \pm 0.1$ ),  $[\alpha/\text{Fe}] = 0.4 \pm 0.1$  ( $0.2 \pm 0.2$ ) and an age of  $13 \pm 2$  ( $11 \pm 3$ ) Gyr. Since the three-dimensional error distributions in the derived parameters are generally asymmetric, uncertainties are taken to correspond to the maximum difference of the parameter in question on the  $1\text{-}\sigma$  surface. Using this fitting procedure, we have derived age,  $[\text{Z}/\text{H}]$  and  $[\alpha/\text{Fe}]$  for the Galactic GC data (P02 and CBR98), and the M31 clusters. The best solutions for age,  $[\text{Z}/\text{H}]$  and  $[\alpha/\text{Fe}]$  for the M31 GCs, using the BC03 and TMB03 models, are given in Table 1. As a result of the  $\chi^2$  fits, several indices were routinely clipped from these datasets, indicating aberrant index values with respect to the stellar population models in question. Specifically, for the M31 data the NaD index was always rejected, and we attribute this to problems with interstellar absorption in this index (e.g., Burstein et al., 1984; TMB03). Furthermore, generally both the  $\text{CN}_1$  and  $\text{CN}_2$  indices were significantly elevated with respect to the model predictions (see later). In

the case of the Milky Way data, again the CN and NaD indices were rejected, as was the Fe5015 index in the P02 data which appears to have calibration issues (see P02 and PFB04). There are four common GCs between the CBR98 and P02 data, and we find encouraging consistency in our solutions between these objects (PFB04). In the following, we use the solutions for the P02 rather than CBR98 clusters in common, since the P02 data generally have more indices available to fit. We refer to these ensemble data as the ‘Galactic GCs’.

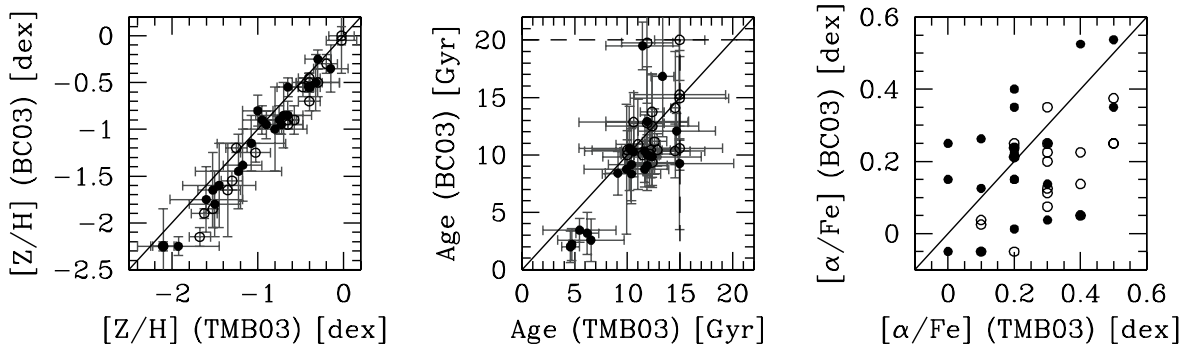


Fig. 8.— Comparison between derived parameters for the Galactic (open circles) and M31 GCs (filled circles) using the Bruzual & Charlot (2003) and Thomas, Maraston & Bender (2003) models. The latter models incorporate higher-order Balmer lines from Thomas, Maraston & Korn (2004). In each panel, the solid line represents unit slope for reference. Error bars have been omitted from the far-right panel for clarity. In general, the agreement between models is acceptable.

Differences between SSP models can be significant, reflecting differing choices made by modelers on issues such as the stellar library, the initial mass function and the choice of isochrone. In Figure 8 we compare the best solutions using the PFB04 method for the BC03 and TMB03 models applied to the Galactic and M31 GCs. The good correlation in metallicity between the BC03 and TMB03 models is very encouraging. However, there is clearly a deviation from unit slope. At the most metal-poor end, the TMB03 models predict metallicities  $\sim 0.25$  dex higher than the BC03 models. This offset decreases at higher metallicities, until no net offset is seen at  $[Z/H] \sim 0$ . In terms of ages, the agreement is also encouraging. Five M31 clusters clearly lie at relatively young ages,  $\sim 6$  (3) Gyr according to the TMB03 (BC03) models. These clusters all have similar metallicities, with  $[Z/H] \sim -1.0$ . A number of GCs also pile-up on the oldest-age line of the TMB03 models, suggesting that their age solutions lie ‘older’ than the models allow. This problem is not seen in the BC03 models, which have a larger age range, although absolute ages of 20 Gyr are inconsistent with the presently favored age of the Universe (Tegmark et al. 2004).

The agreement between the  $[\alpha/Fe]$  ratios is less convincing, although a correlation is present.

The BC03 models predict  $[\alpha/\text{Fe}]$  ratios  $\sim 0.15$  dex lower than TMB03 for the Galactic GC data. In correcting for the local abundance pattern in the BC03 models, we have assumed the same pattern as that adopted by TMB03, which shifts from  $[\alpha/\text{Fe}]=+0.25$  at  $[\text{Z}/\text{H}]=-2.25$  to  $[\alpha/\text{Fe}]=0$  at  $[\text{Z}/\text{H}]=0$ . This is quite a low value to adopt, when one considers that  $[\alpha/\text{Fe}]=0.4\sim 0.6$  is more in keeping with the local stellar abundance pattern of (for example)  $[\text{O}/\text{Fe}]$ ,  $[\text{Mg}/\text{Fe}]$  and  $[\text{Ca}/\text{Fe}]$  at  $[\text{Fe}/\text{H}]\leq -1$  (see Gratton et al. 2004 and references therein). The  $[\alpha/\text{Fe}]$  pattern adopted by TMB03 reflects the mean of  $[\text{Mg}/\text{Fe}]$  and  $[\text{C}/\text{Fe}]$  observed in the solar neighborhood, which are  $\sim 0.4$  and  $\sim 0.1$  respectively (at  $[\text{Fe}/\text{H} < -1]$ ), and therefore presumably reflects  $[\text{Mg}+\text{C}/\text{Fe}]$ . To maintain consistency with TMB03, we adopt their values for this correction.

In summary, there is generally acceptable agreement between the predictions of the BC03 and TMB03 models. Of the three key parameters we are interested in, the reliability of the predicted  $[\alpha/\text{Fe}]$  ratios are the least convincing. Since the derived parameters are still somewhat model-dependent, we will explicitly state which model was used when quoting values for age, metallicity and abundance ratios. We emphasize that the ages, metallicities and abundance ratios discussed in the following sections do not explicitly take into account the intrinsic uncertainties in the stellar population models used. Moreover, absolute values, particularly for ages, should be treated with caution.



### 4.3. Globular Cluster Ages, Metallicities and Abundance Ratios

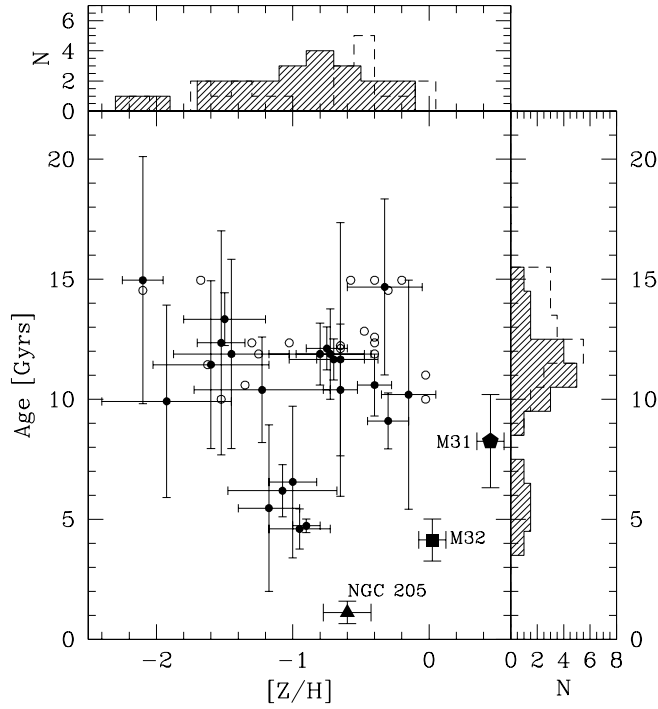


Fig. 9.— The ages and metallicities of the M31 (filled circles with errors), and Galactic GCs (open circles) according to the Thomas, Maraston & Bender (2003) models. The shaded and open-dashed histograms exclusively represent the M31 and Galactic GCs respectively. Also shown are the positions of NGC 205, M32 and the bulge of M31, data taken from Trager et al. (1998).

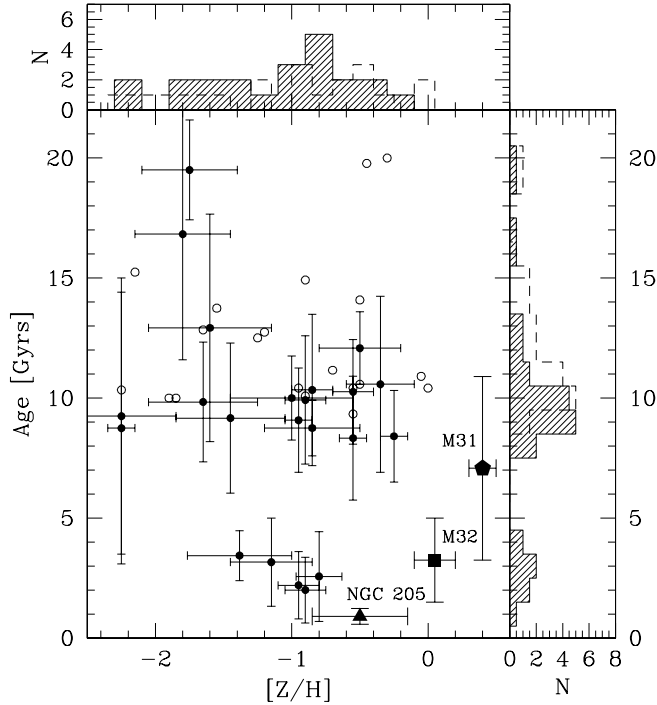


Fig. 10.— The ages and metallicities of the M31 and Galactic GCs according to the Bruzual & Charlot (2003) models. Symbols as for previous figure.

Our best-fit ages and metallicities for the GCs are shown in Figures 9 and 10. Although in detail, the ages and metallicities derived from the TMB03 and BC03 models differ, the basic conclusions remain the same. The M31 GCs separate out into three clear groupings: a metal-poor, old component (7 clusters), a metal-rich, old component (10 clusters) and an intermediate age, intermediate-metallicity component (5 clusters). Reassuringly, all the Galactic GCs are 10 Gyr old or older according to both sets of models. As mentioned previously, the intermediate age GCs (henceforth IAGCs) lie at around  $\sim 5$ -6 Gyrs according to the TMB03 models, whereas the BC03 models put them at 2-3 Gyrs old. Their ages and metallicities are not dissimilar to those observed for star clusters in the Small Magellanic Cloud (SMC; e.g., Da Costa & Hatzidimitriou 1998). Broad-band optical colors are affected by age-metallicity degeneracy and uncertain reddenings. However, the colors of the intermediate age candidates support our spectroscopic findings (Section 4.4). Excluding cluster NB 16, which possesses  $B-V=1.33$  and we believe is highly reddened, we obtain  $\langle(B-V)_0\rangle=0.7\pm 0.1$ . Assuming a metallicity of  $[Z/H]=-1.0$ , this corresponds to ages of roughly 5 Gyrs according to the BC03 and Maraston (1998) models.

The right-hand panels of Figures 9 and 10 clearly show that the age distribution in the M31

GCs is bimodal, whereas this is not the case for the Galactic GCs. Intriguingly, there is also evidence that the mean ages of the old GCs are different between the M31 and Galactic samples. The old M31 GCs appear to be on average  $\sim 2$  Gyr younger than the Galactic GCs, and this is driven by the metal-rich ( $[Z/H] > -1.0$ ) M31 clusters. Since these are differential comparisons, and are seen in the results for both models, this is a fairly robust result. However, the analysis of a larger, unbiased sample of clusters is required to check the reality of this result. The metallicity distributions of the two GC samples appear quite similar, although the Galactic GC sample extends to slightly higher metallicities. We identified no super-solar metallicity M31 GCs in our sample. One M31 GC in our sample, 225-280, possesses CMDs obtained with HST/WFPC2 (Fusi-Pecci et al. 1996) and HST/NICMOS (Stephens et al. 2001). Our metallicity for this GC is TMB03 (BC03)  $[Z/H] = -0.3 \pm 0.15$  ( $-0.25 \pm 0.10$ ). The two HST studies are in good agreement, with  $[Z/H] = -0.4$  and  $-0.15 \pm 0.37$  respectively.

Also indicated in Figures 9 and 10 are the positions of NGC 205, M32 and the bulge of M31 (using the data of Trager et al. 1998). The M31 bulge is clearly much more metal-rich than both GC samples, whereas M32 appears to have a metallicity comparable to the most metal-rich Galactic bulge clusters NGC 6553 and NGC 6528. Our ages and metallicities for both M31 and M32 are consistent with previous findings (e.g. Mould, Kristian & Da Costa 1984; Terlevich & Forbes 2002; Schiavon et al. 2004a). In terms of age and metallicity, the IAGCs are closer to that of the dwarf elliptical NGC 205. Our solutions for NGC 205 indicate that it is both slightly more metal-rich ( $[Z/H] = -0.8$  (TMB03)), and somewhat younger than ( $\sim 1$  Gyr) the IAGCs. This seems to suggest either very recent or ongoing star formation in this galaxy (Bica et al. 1990; Lee 1996; Demers, Battinelli & Letarte 2003).

On the CN abundances of these data, as discussed in Section 4.1, the Milky Way and majority of M31 clusters are strongly overabundant in the Lick CN indices when compared to SSP models based on local stars. This is confirmed during the  $\chi^2$  fitting procedure. The CN indices are rarely able to be fit when the best solutions for age, metallicity and abundance ratio are found (see also PFB04). This is also true for the bulge of M31, which appears to be at least as overabundant in CN as the M31 and Galactic GCs. However, this is *not* the case for any of the IAGCs, NGC 205 or M32 (see also Schiavon et al. 2004a). Since the CN index does not evolve strongly with age, particularly after a few Gyr, this result implies that these objects do not exhibit any significant CN-enhancement.

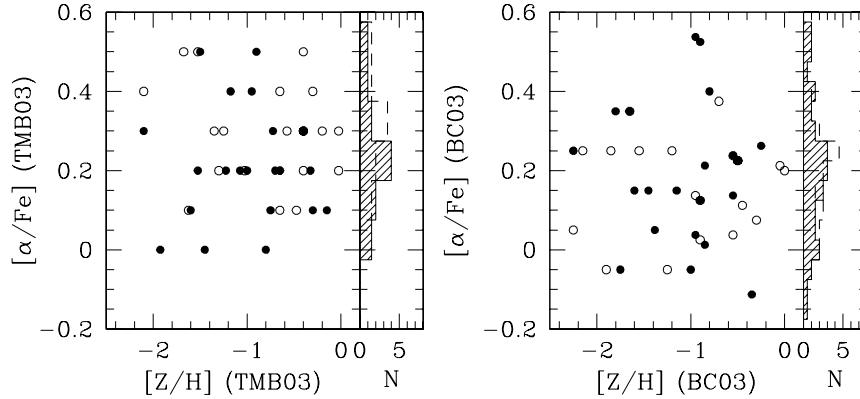


Fig. 11.— The behavior of  $[\alpha/\text{Fe}]$  with  $[\text{Z}/\text{H}]$  for the M31 and Galactic GCs as inferred from the Thomas, Maraston & Bender (2003) and Bruzual & Charlot (2003) models. Symbols are as for the previous figure. No significant trend is seen with metallicity.

The behavior of  $[\alpha/\text{Fe}]$  with  $[\text{Z}/\text{H}]$  for the GCs is shown in Figure 11. The vast majority of GCs exhibit  $[\alpha/\text{Fe}] > 0$ , which is consistent with Figure 1. There is no clear trend with metallicity; the Galactic and M31 GCs appear to be similarly enhanced at all values of  $[\text{Z}/\text{H}]$ . Interestingly, the TMB03 models suggest that the Galactic GCs are some  $\sim 0.1$  dex more enhanced in  $[\alpha/\text{Fe}]$  than the M31 GCs (c.f. Figure 1). However, this is not supported by the BC03 models which suggest similar levels of enhancement between the two populations. Therefore, in this regard, it is difficult to come to significant conclusions. We have also determined  $[\alpha/\text{Fe}]$  ratios using the TMB03 (BC03) models for NGC 205, M32 and M31 and find  $[\alpha/\text{Fe}] = -0.3 \pm 0.1 (-0.3 \pm 0.1)$ ,  $-0.1 \pm 0.1 (0 \pm 0.1)$  and  $0.2 \pm 0.1 (0.1 \pm 0.1)$  respectively. These values are consistent with previous studies based upon integrated spectra (Terlevich & Forbes 2002; Schiavon et al. 2004a).

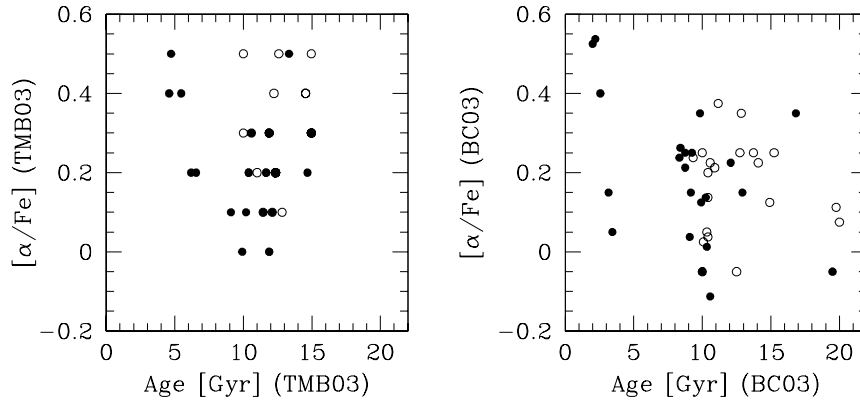


Fig. 12.— The behavior of  $[\alpha/\text{Fe}]$  with age for the M31 and Galactic GCs as inferred from the Thomas, Maraston & Bender (2003) and Bruzual & Charlot (2003) models. Symbols are as for the previous figure. The IAGCs appear to have significant  $[\alpha/\text{Fe}]$  enhancement.

Figure 12 shows the behavior of  $[\alpha/\text{Fe}]$  with GC age. The IAGCs seem to have on average higher  $[\alpha/\text{Fe}]$  ratios than the old GCs using both models. A Kolmogorov-Smirnov test finds that this is significant at the  $2\sigma$  level. This may suggest that the material from which these objects formed was preferentially exposed to the ejecta from type-II supernovae, similar to the situation for young clusters in the merger remnant NGC 3610 (Strader et al. 2004). The  $\alpha$ -abundance pattern at  $[\text{Z}/\text{H}] \sim -1.0$  is consistent with that seen for intermediate age Large Magellanic Cloud (LMC) clusters (R. Proctor, private comm.). The TMB03 models suggest a slight correlation between age and  $[\alpha/\text{Fe}]$  for the old M31 GCs, in the sense that the  $[\alpha/\text{Fe}]$  ratios are lower for younger clusters. This is, however, not apparent in BC03 model predictions.

In summary, we find that the M31 GCs in our sample separate into three distinct groups in age and metallicity. We identify an old, metal-poor group, an old metal-rich group and an intermediate age, intermediate metallicity group. This result does not depend upon the SSP model employed. The  $[\alpha/\text{Fe}]$  ratios of the M31 GCs are somewhat more model-dependent, but in general we find that the GCs have  $[\alpha/\text{Fe}] > 0$  similar to, perhaps slightly lower than, the Galactic GCs. The IAGCs appear strongly enhanced in  $\alpha$ -elements.

#### 4.4. The Nature of the Intermediate-Aged Clusters

Previous spectroscopic studies of M31 GCs have indicated that photometric catalogs of M31 GCs can suffer from contamination due to foreground stars (e.g., Barmby et al. 2000; Perrett et al. 2002). Kinematics of the M31 GCs does not uniquely determine their identity, since the velocity fields of both the Galactic stellar disk and halo overlap with the M31 GC velocity distribution. For

example, at the Galactic co-ordinates of M31 ( $l=121.17^\circ$ ,  $b=-21.57^\circ$ ) foreground disk F-dwarfs are expected to have a mean streaming velocity of  $\sim -62 \text{ kms}^{-1}$  according to the Besançon<sup>8</sup> Galactic model (Robin et al. 2003). In terms of visual identification, due to the proximity of M31 ( $D\sim 780 \text{ kpc}$ , Holland 1998; Stanek & Garnavich 1998), GCs are only distinguishable from stars from the ground in sub-arcsecond seeing conditions. In view of this, it is important to ask whether the IAGCs we have identified are truly clusters in M31, rather than foreground disk or halo stars.

Two of the IAGCs, 292-010 and 337-068, have been partially resolved by Racine (1991) using high-resolution CCD imaging. He identifies these as *bona fide* clusters and we have no reason to doubt these identifications. The catalogs of Battistini et al. (1993,1987) and Sargent et al. (1977) have been shown to be partially contaminated with foreground stars and galaxies (e.g. Barmby et al. 2000). These photometric studies include the IAGCs 126-184, 301-022, NB16 and NB67. We searched for archival ground-based CCD imaging with sub-arcsecond seeing and an adequate pixel scale, and found I-band imaging for IAGCS 126-184, 301-022 and NB16 in the NOAO NSA archives (M31F5-I and M31F9-I, PI Dr P. Massey)<sup>9</sup> taken with the Kitt Peak National Observatory 4-m 8K $\times$ 8K Mosaic-1 CCD. From measuring the point-spread functions (PSFs) of several stars in the images we determined the seeing to be 0.7 arcsec and 0.9 arcsec for the F5-I and F9-I fields respectively. We checked and verified that these PSFs did not vary significantly across the field of view of these data.

---

<sup>8</sup>[bison.obs-besancon.fr/modele/](http://bison.obs-besancon.fr/modele/)

<sup>9</sup>[archive.noao.edu/nsa](http://archive.noao.edu/nsa)

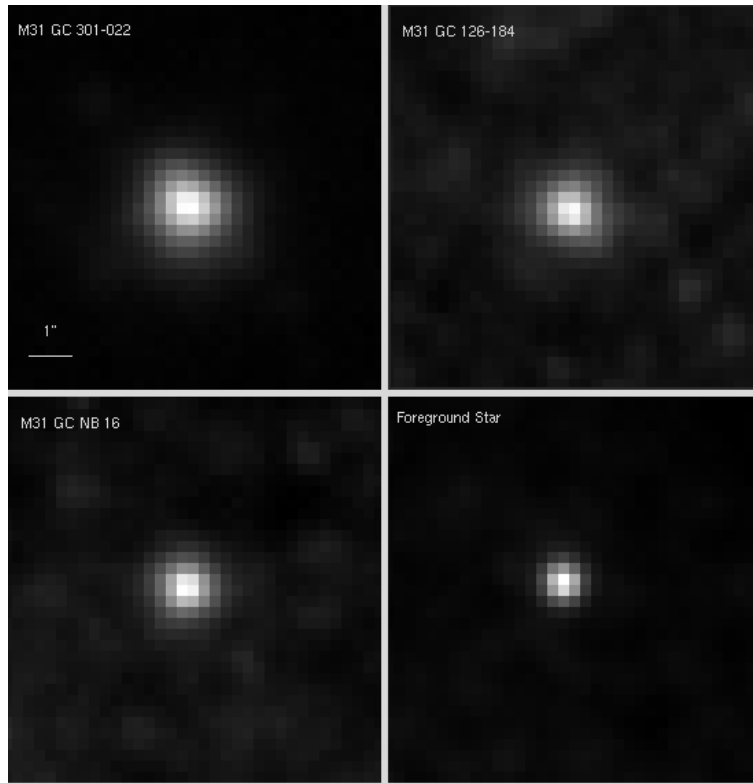


Fig. 13.— KPNO Mosaic-1 I-band images of the IAGCs 301-022, 126-184 and NB16. The images are  $9 \times 9$  arcsec, and the pixel scale of the KPNO images is 0.258 arcsec/pixel. Also shown is the appearance of a foreground star identified from the USNO-A2.0 astrometric catalog, which has a similar I-band magnitude to the IAGCs. The same logarithmic image scaling and intensity cuts have been applied in each case. The IAGCs are clearly less centrally concentrated than the star.

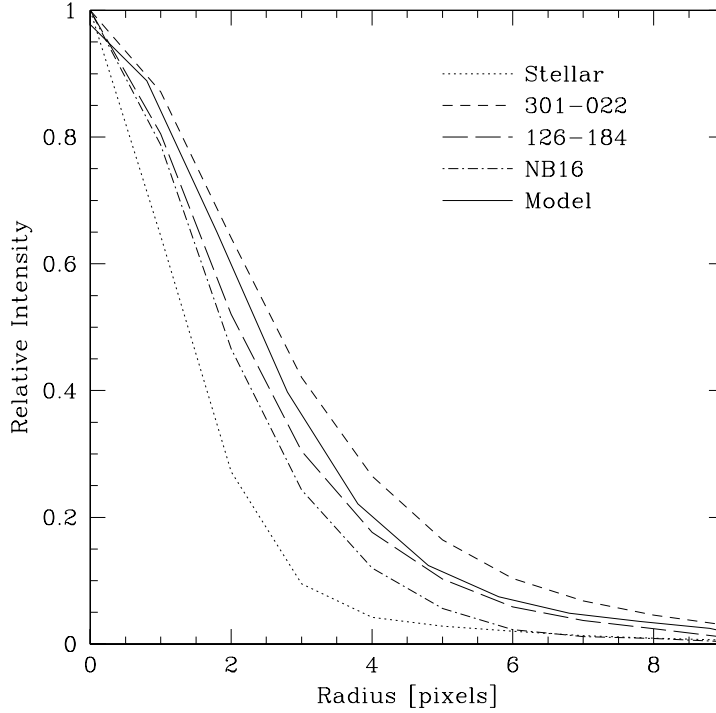


Fig. 14.— Radial brightness profiles of the IAGCs 301-022, 126-184 and NB16 compared to the comparison star shown in the previous figure. All three IAGCs appear non-stellar. Also shown is the profile of an artificial globular cluster at the distance of M31, convolved with a Gaussian PSF (see text).

Postage-stamp images of the three IAGCs taken from the KPNO frames are shown in Figure 13. The three clusters clearly appear more extended, and less centrally peaked, than the comparison star. This is confirmed by the radial profiles of these objects which are shown in Figure 14. In each case, the IAGCs show an excess of light beyond the PSF expected of a foreground star. For comparison, we also show the brightness profile of an artificial GC with a Hubble profile (core radius of 0.2 pc), which has been convolved with a Gaussian PSF of 0.7 arcsec and placed at the distance of M31. We conclude that these are non-stellar objects with sizes consistent with compact globular clusters.



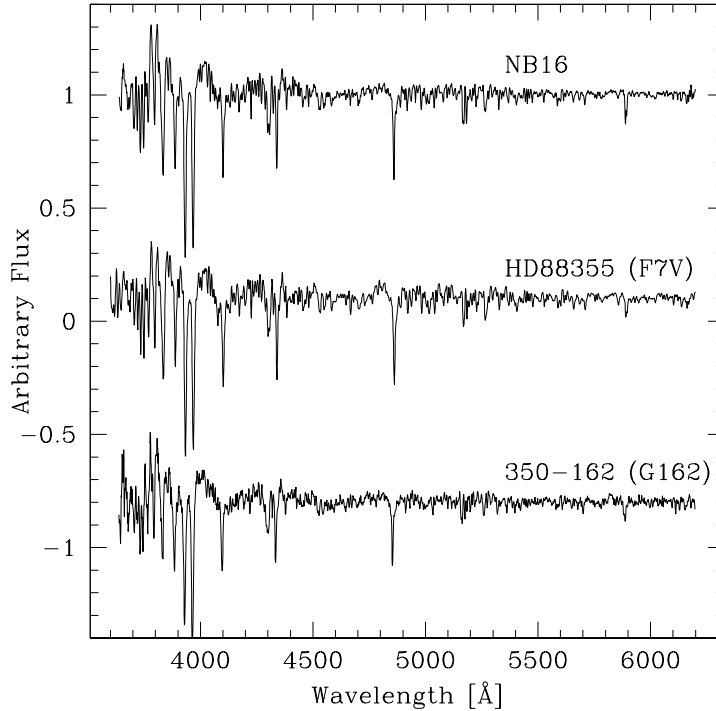


Fig. 15.— Normalized spectra for a candidate IAGC (NB16; top), a Galactic F-dwarf from the STELIB library (Le Borgne et al. 2003) and a true metal-poor, old M31 GC (350-162; bottom).

By cross-correlation with the STELIB stellar library (Le Borgne et al. 2003) and through visual inspection, we assign spectral types to the IAGCs of F6–F7. Both strong Balmer lines and metallic lines are visible characteristics of these spectral types. In Figure 15 we compare the spectra of a candidate IAGC (NB16) with that of a Galactic F-dwarf taken from the STELIB library and an old, relatively metal-poor ( $[Z/H] \sim -1.5$ ) M31 GC (350-162). All three objects exhibit F-type spectra and look quite similar. The ‘inversion’ of the Ca II H&K lines indicates the presence of a hotter population of stars in the spectrum of 350-162, which are presumably horizontal branch stars (see Section 5). NB16 and the Galactic F7 dwarf HD 88355 appear very similar; one difference is the stronger strontium line ( $\lambda 4077$ ) in the Galactic dwarf indicating metallicity and/or luminosity differences.

Further, indirect evidence for the cluster nature of the IAGCs comes from optical/near-IR colors, which potentially discriminate between warm stars and intermediate age stellar populations; the latter are expected to be redder in near-IR passbands for a given optical color due to the flux contribution from cooler stars on the giant branch (see e.g., Puzia 2003).

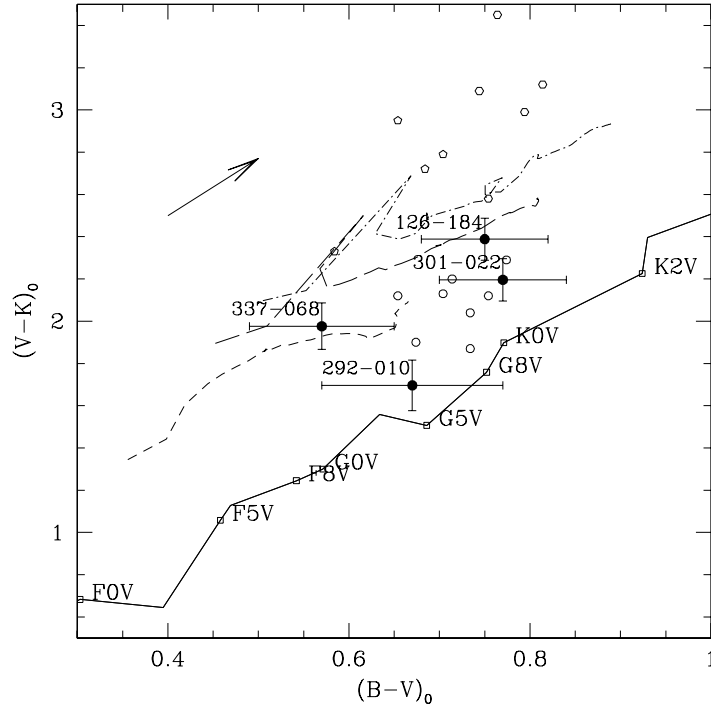


Fig. 16.— Colors of four IAGC candidates (126-184, 301-022, 337-068 & 292-010) for which exist optical and near-IR photometry. Open symbols are for LMC clusters (circles: SWB type VII; hexagons: SWB VI; pentagons: SWB V) taken from Persson et al. (1983) and Bica et al. (1996). Also shown is the stellar sequence for F-K dwarfs in the solar neighborhood. Short-dashed, long-dashed and dash-dotted lines represent metallicities  $[Fe/H] = -1.65, -0.64$  and  $-0.33$  respectively for ages 1–20 Gyr from Bruzual & Charlot (2003). The arrow corresponds to a reddening of  $E(B-V)=0.1$  ( $E(V-K)=0.27$ ). Three of the IAGCs lie clearly above the stellar sequence.

The  $(B-V)_0, (V-K)_0$  colors for four IAGCs for which we have optical and near-IR photometry are shown compared to the local stellar sequence in Figure 16. For clusters 126-184 and 337-068 we do not have reliable reddening estimates and therefore have assumed a mean  $E(B-V)=0.22$  (Barmby et al. 2000). Three IAGCs (126-184, 301-022 & 337-068) lie 0.3–0.5 mag above the stellar locus; this cannot be attributable to reddening since this vector runs parallel to this locus. The IAGC candidate 292-010 lies near the stellar locus, although as noted previously Racine (1991) identified this as a partially resolved object. We also show in the figure the positions of LMC clusters with SWB types V, V and VII (corresponding to ages 0.8–2, 2–5 and 5–16 Gyr respectively; Bica et al. 1992). With the exception of 292-010, the IAGCs lie somewhere between the old (SWB VII) and younger (SWB V and VI) clusters, consistent with our age estimates.

A schematic of how the M31 GCs in our sample are distributed with respect to the optical

disk of M31 is shown in Figure 17. The old M31 GCs are widely distributed across the optical disk and halo, and exhibit rotation in the sense of NE-approaching and SW-receding. This is consistent with the Perrett et al. (2002) results for a larger sample of GCs. Rotation in the young ( $\leq 1$  Gyr) metal-rich ( $[Z/H] \sim 0$ ) disk clusters (Morrison et al. 2004; Paper I) is also apparent in Figure 17. Three of the IAGCs (126-184, NB16 and NB67) are located near the bulge regions of M31, and have comparable velocities ( $-182 \pm 14$ ,  $-115 \pm 15$  and  $-113 \pm 17$   $\text{kms}^{-1}$  respectively). The three other IAGCs (292-010, 301-022 and 337-068) show no preferred spatial distribution, and have disparate velocities ( $-392 \pm 56$ ,  $-30 \pm 30$  and  $50 \pm 12$   $\text{kms}^{-1}$  respectively). The IAGCs show no signs of rotation but, excluding 292-010, do exhibit higher velocities than the bulk of the M31 GC system (see Figure 18).

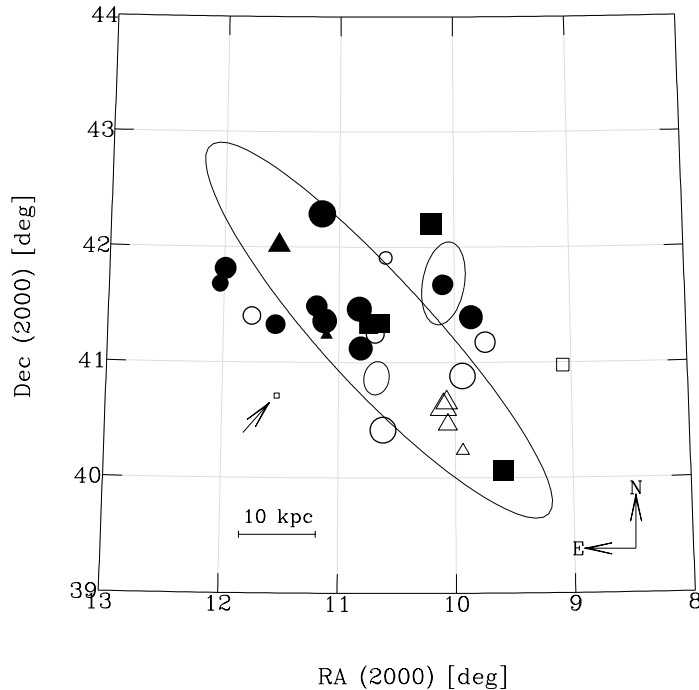


Fig. 17.— Spatial distribution of M31 GCs, with respect to the M31 disk (large ellipse), NGC 205 (ellipse N of disk) and M32 (small ellipse). Open symbols for old (open circles) and intermediate age GCs (open squares) represent velocities lower than M31 systemic velocity ( $-300$   $\text{kms}^{-1}$ ). Filled symbols indicate velocities higher than this, with symbol size proportional to the velocity residual from the systemic velocity. Note that three IAGCs are stacked in the central regions, and have been offset slightly for display purposes. Also shown are the young disk clusters identified in Paper I (open and filled triangles) and the ACS field of Brown et al (2003; indicated by an arrow).

The velocity distribution of the M31 sample is shown in Figure 18. The mean velocity of our entire sample (including the disk clusters - Paper I) is  $-275 \pm 28$   $\text{kms}^{-1}$ , with a velocity dispersion of

155  $\text{kms}^{-1}$ . Excluding 292-010, the mean velocity of the IAGCs is  $-78 \pm 36 \text{ kms}^{-1}$ , with a velocity dispersion of  $80 \text{ kms}^{-1}$ . Monte Carlo tests by drawing velocities randomly from the parent velocity distribution indicate that this velocity difference is statistically significant at the 99.8% confidence level. Also shown in Figure 18 is the velocity distribution for  $\sim 200$  clusters from Perrett et al. (2002). Comparison between the velocity distribution of the full M31 sample and that of Perrett et al. (2002) suggests that we are probably missing a number of lower velocity GCs ( $\sim -400 \text{ kms}^{-1}$ ).

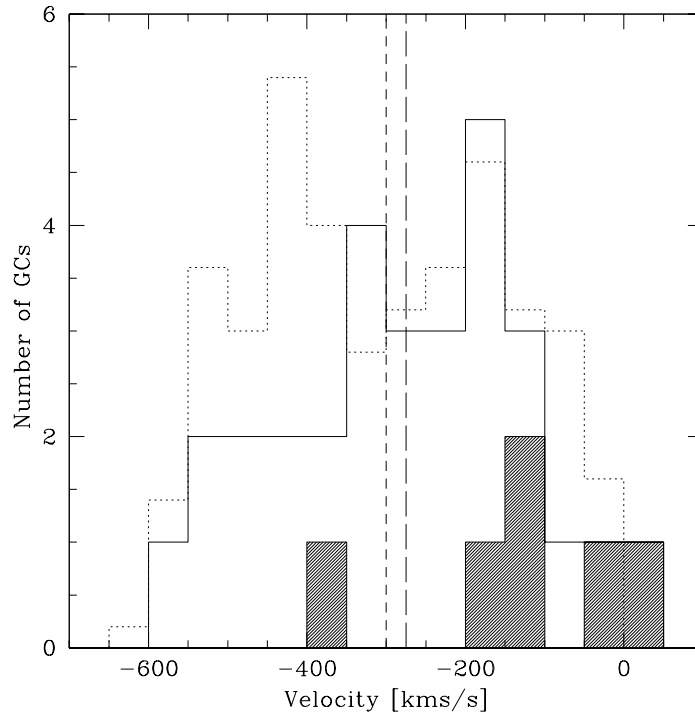


Fig. 18.— Velocity distribution of M31 GCs. The filled histogram indicates the velocities of the IAGCs, the open histogram is for our full sample. The dotted histogram is for the sample of  $\sim 200$  GCs from Perrett et al. (2002) scaled down by a factor of 6. The vertical short-dashed line indicates the systemic velocity of M31 ( $-300 \text{ kms}^{-1}$ ), the vertical long-dashed line indicates the mean velocity ( $-275 \pm 28 \text{ kms}^{-1}$ ) of our full sample.

In summary, based upon the extended nature and colors of the IAGCs, we conclude that clusters 126-184, 292-010, 301-022, 337-068 & NB16 are star clusters associated with M31. At present we cannot state confidently that NB67 is also a star cluster, although its similarity to NB16 in terms of line-strengths and kinematics makes this a distinct possibility.

## 5. The Horizontal Branch Morphologies of M31 GCs

Age estimates based on Balmer lines can be seriously affected by the presence of blue horizontal branches (HBs) in GCs (Lee et al. 2000; Beasley et al. 2002; Peterson et al. 2003; TMB03; Schiavon et al 2004b). Such stars have high temperatures, and can mimic the effect of hotter (younger) turn-off temperatures. The existence of varying HB morphology at a given metallicity in some GCs (the second parameter effect) further complicates this issue (e.g., TMB03). We can, however, rule out the possibility that hot HB stars are conspiring to make the IAGCs look young in their integrated spectra through three arguments:

Firstly, the multivariate approach which we have employed is robust against such a possibility. This has been demonstrated by PFB04, and is essentially true because reliable age estimates can be determined without the use of Balmer lines in the age determination. This can be achieved because each index retains some age and metallicity information. By using sufficient indices, the age-metallicity degeneracy can be broken without the use of the age-sensitive Balmer lines. Since these indices are the most temperature sensitive (and hence HB morphology sensitive) Lick indices, omitting these from the  $\chi^2$  fit allows the potential effects of HB stars to be mitigated.

Secondly, Schiavon et al. (2004b) have shown that the age-HB morphology degeneracy can be broken by comparing the strengths of the Balmer lines. They argue that bluer Balmer lines should be effected more strongly by the presence of blue HB stars because at the characteristic temperatures of such stars ( $\sim 9000\text{K}$ ), their relative flux contribution increases for bluer indices. Thus,  $H\delta$ ,  $H\gamma$  should be relatively stronger than  $H\beta$  in the integrated spectrum of an HB-affected GC, when compared to a canonical model grid. Inspection of Figures 3, 4 and 5 indicates that this is not the case here, in fact the  $H\beta$  index appears much stronger in the IAGCs relative to the older M31 clusters than do the higher-order Balmer lines. Conversely, this difference in separation between  $H\beta$  and the higher-order Balmer lines could be qualitatively explained if one assumes that the IAGCs have purely red HBs, and the Balmer lines of the 'old' metal-poor GCs are affected by HBs. However, then the only explanation for the position of the IAGCs in the  $H\beta$ -[MgFe] plane (Figure 3) is to invoke intermediate ages.

Thirdly, we may estimate the HB morphology of the M31 GCs by using the Rose (1984) Ca II diagnostic (see also Tripicco 1989; PFB04). The Ca II index, defined as the ratio of the Ca II H+He to Ca II K line, is sensitive to the presence of hot stars in evolved stellar populations (Rose 1985). This index is extremely effective in identifying hot stellar populations because it is a ratio of two strong lines of singly ionized calcium, which implicitly arise from the same physical process. Since He is coincident (in wavelength) with the Ca II H line, hot stellar populations will strengthen this line without effecting Ca II K. As shown by PFB04, this index shows a remarkable correlation with horizontal branch (HB) morphology; Ca II increases as HBs become bluer due to the strengthening of Ca II H+He relative to Ca II K.

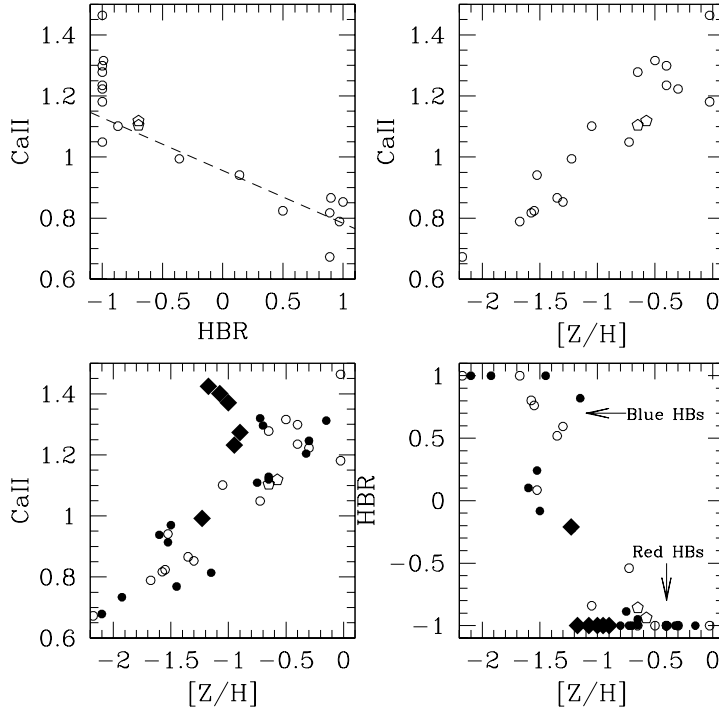


Fig. 19.— Calibration of the Rose (1984) Ca II index for horizontal branch morphology. The top-left panel shows the good correlation between the horizontal branch parameter and the Ca II index for Galactic GCs (open symbols). The two open pentagons represent the Galactic GCs NGC 6388 and NGC 6441, which are metal-rich but are known to contain a blue HB component (Rich et al. 1997). The dashed line is a fit to these data (see text). The large solid diamonds indicate the IAGCs. The top-right panel shows the correlation between Ca II and our derived metallicities for the Galactic GCs using the Thomas, Maraston & Bender (2003) models. The bottom-left panel shows the same correlation, but includes the M31 GCs (solid symbols). The bottom-right panel shows our derived HB morphology for all the GCs.

Figure 19 shows the calibration of the HB parameter (Lee et al. 1994) for the Milky Way and M31 GCs. We have measured the Ca II index for the P02 and M31 data, the former which we have augmented with data for seven additional Galactic GCs (47 Tuc, NGC 362, NGC 1466, NGC 1851, NGC 1904, NGC 6652 and NGC 7099) described in Gregg (1994). Seven clusters are in common between the P02 and full Gregg (1994) sample, and we find excellent agreement; (P02-Gregg)=0.012,  $\sigma=0.062$  in Ca II between the two. The HB parameter is taken from the Harris (1996) catalog in all but one case; NGC 1466 in the Gregg (1994) sample. This is actually an LMC cluster for which we adopt the HB ratio in Johnson et al. (1999). The top-left panel in Figure 19 illustrates the good correspondence between Ca II and the HB parameter. Unfortunately the HB parameter saturates before Ca II, however, blue HBs can clearly be separated from red HBs, while intermediate HB morphologies may be estimated.

We calibrate the Ca II index to indicate HB morphology as:

$$\text{HBR} = \begin{cases} +1, & \text{Ca II} \leq 0.6 \\ -4.99 \times (\text{Ca II}) + 4.77, & 0.6 < \text{Ca II} < 1.2 \\ -1, & \text{Ca II} \geq 1.2 \end{cases}$$

where  $\text{HBR}=-1$  is equivalent to purely red HBs,  $+1$  equivalent to purely blue HBs and intermediate values corresponding to intermediate HB morphologies. Our measured values for Ca II, and the corresponding values for the HB parameter for the M31 GCs are listed in Table 1.

Figure 19 (bottom-left) compares the the Ca II index with our derived (TMB03) metallicities for the Galactic and M31 GCs. The correlation is good, with the exception that the IAGCs which generally have too high Ca II for their metallicities. The bottom-right panel shows the HB ratio, derived from Ca II, versus (TMB03) metallicity. We find using the BC03 metallicities yields similar results in this calibration. The M31 GCs clearly possess a range of HB morphologies, from very blue, to intermediate morphologies, to very red. The majority appear to possess purely red HBs, which is consistent with recent GALEX UV measurements (M. Rich, private comm.). All but one of the IAGCs are included in this category. IAGC 292-010 shows evidence for an ‘intermediate’ HB morphology.

Two Galactic GCs which are metal-rich, but exhibit blue HB components (Rich et al. 1997), are indicated in Figure 19. These clusters lift slightly from the ‘pure red HB’ value of  $\text{HBR}=-1$ . This suggests that the Ca II method is sensitive to such populations. Two M31 GCs also show similar behavior, 158-213 and 234-290, and are candidate metal-rich GCs in M31 which may have blue HB components. Clearly this latter effect only weakly registers in Ca II, and therefore relatively reliable metallicity estimates are required for it to be successful.

Based upon the previous arguments, we conclude that it is unlikely that blue HBs are having a significant impact upon our age (or metallicity) determinations, and that the IAGCs possess intermediate ages, rather than old ages and blue horizontal branches.

## 6. Discussion

Using the stellar population models of Bruzual & Charlot (2003) and Thomas, Maraston & Bender (2003) we have estimated metallicities, ages and  $[\alpha/\text{Fe}]$  ratios for 21 globular clusters in the Milky Way and 23 globular clusters in M31. Our principle findings are as follows:

- as expected, we find that the Milky Way clusters are uniformly old (within our measurement uncertainties), span a metallicity range,  $-2.0 \leq [\text{Z}/\text{H}] \leq 0$ , and have mean  $[\alpha/\text{Fe}]$  ratios of  $0.2 \sim 0.4$  (depending upon the models employed).

- the M31 clusters span a very similar metallicity range to the Milky Way clusters, and are also enhanced in  $\alpha$ -elements. There is some evidence that the old, metal-rich ( $[Z/H] > -1.0$ ) clusters in M31 are  $\sim 2$  Gyr younger than the equivalent Milky Way GCs, although a larger sample of M31 GCs will test the validity of this result.
- there is weak evidence that the M31 clusters have lower  $[\alpha/Fe]$  ratios than their Milky Way counterparts. We see no evidence for a correlation between  $[Z/H]$  and  $[\alpha/Fe]$ .
- M31 has a population of intermediate age (2–6 Gyr), intermediate-metallicity ( $[Z/H] \sim -1.0$ ) globular clusters (IAGCs). Through consideration of high-resolution CCD imaging and optical/near-IR colors for a subset, we show that it is unlikely these objects are interloping foreground stars.
- stellar population models suggest that these IAGCs exhibit  $\langle [\alpha/Fe] \rangle \sim 0.3\text{--}0.5$ , and, with the exception of one cluster identified in Paper I, possess higher velocities than the bulk of the M31 cluster sample. Three of the IAGCs are concentrated in the bulge regions of M31, the remaining three lie in the 'halo' regions.
- when compared to the rest of the M31 and Milky Way sample, the IAGCs have low CN values. Furthermore, the IAGCs appear to be 'CN-depressed' with respect to stellar population models.

Although our sample of M31 GCs is not unbiased, the implications of the relative numbers of cluster sub-populations identified in our spectroscopic sample are surprising. Including the six young disk clusters identified in Paper I (and excluding Hubble V in NGC 205), from a total sample of 29 M31 globular clusters: 17 ( $\sim 58\%$ ) are old (metal-poor and metal-rich), 6 ( $\sim 21\%$ ) are intermediate age and intermediate-metallicity and 6 ( $\sim 21\%$ ) are metal-rich, young disk clusters. van den Bergh (1999) estimated that the total population of M31 GCs is  $400 \pm 55$ , with 337 confirmed GCs (Galleti et al. 2004). Using the estimates of van den Bergh, 232  $\pm$  32 GCs in M31 are old (metal-poor and metal-rich), and there are 84  $\pm$  12 intermediate age globular clusters, with a similar number of young disk clusters. This is highly likely to be a significant overestimate, and a complete spectroscopic sample of M31 GCs is required in order to check these crude values.

It is, at present, unclear whether the disk clusters are truly globular clusters, or simply represent the upper end of the open cluster luminosity function (Paper I). However, the IAGCs have luminosities (and hence masses, accounting for age-fading) consistent with normal globular clusters ( $15.3 \leq V_0 \leq 17.5$ ;  $4 \times 10^4 \leq L_{GC} \leq 5 \times 10^5 L_{\odot}$ ). The spatial distribution of the IAGCs hints that any globular cluster formation which may have occurred 2–6 Gyr ago in M31 was not confined to the bulge regions of this Galaxy. This suggests that the formation of the IAGCs cannot be explained by secular evolution in the inner-disk/bulge regions (e.g., Maoz et al. 2001), without some mechanism for transporting a significant fraction out to large radii.

Interestingly, although unfortunately not included in the present sample, there is evidence to suggest that several of the outer halo Milky Way GCs may be younger than their inner-halo



counterparts. For example, color-magnitude diagrams have suggested that the outer halo GCs Pal 12 (Gratton & Ortolani 1988; Stetson et al. 1989; Rosenberg et al. 1998) and Ruprecht 106 (Buonanno et al. 1990; Da Costa et al. 1992; Buonanno et al. 1993) may have ages up to 30% younger than old halo GCs (i.e., as young as  $\sim 8$  Gyr). It has been suggested that Pal 12 could have been captured from the Sagittarius dwarf spheroidal (Sgr dSph) (Irwin 1999), and this notion is supported by the fact that Pal 12 lies among the tidal debris presently being stripped from the Sgr dSph (Martinez-Delgado et al. 2002; Bellazzini et al. 2003). Further evidence for this idea comes from the  $\alpha$ -capture elements of Pal 12 (Brown et al. 1997; Cohen 2004) and Rup 106 (Brown et al. 1997), which do not appear to be enhanced with respect to the solar values, but are consistent with the abundances of Sgr dSph stars (Bonifacio et al. 2000; Smecker-Hane & McWilliam 2002). It is possible, although at present speculative, that the intermediate-aged clusters we have identified in M31 are younger analogs of these Milky Way GCs.

Observations of stellar substructure in M31 (e.g., Ibata et al. 2001; McConnachie et al. 2004), suggest that mergers and/or accretions have played an important role in the growth of M31’s halo stellar populations. One possibility is that M31 underwent a major merger  $\sim 6$  Gyr ago ( $z \sim 0.6$  for a standard flat cosmology), forming GCs and field stars in the process. Indeed, Brown et al. (2003) have presented evidence for an intermediate age (6–8 Gyr) population of stars in the halo of M31, which they argue may hint at such an event. During such a merger, any pre-existing metal-rich stellar component (e.g., bulge or thick-disk stars) is expected to be partly redistributed to large radii as observed in M31’s halo. The putative thin-disk in M31 (Morrison et al. 2004) is not a strong constraint on the nature of the hypothetical merger, since the disk may in fact be rather young ( $\sim 1$  Gyr, Paper I). A  $\sim 6$  Gyr hiatus is potentially sufficient time for shocked gas to cool into a new disk configuration.

However, the relatively low metallicities of the IAGCs makes a major merger origin look somewhat unlikely, unless the merger progenitors were surprisingly metal-poor. The merging of two present-day  $L_*$  spirals is expected to produce rather metal-rich ( $[Z/H] \geq 0$ ) field stars and star clusters (Bekki et al. 2002). Such major merging has to occur relatively early in order to reproduce the red peak of elliptical galaxy GC systems (Beasley et al. 2002). An additional constraint is that the  $[\alpha/Fe]$  ratios of the IAGCs imply that the proto-IAGC clouds were preferentially enriched by Type-II supernovae. This abundance pattern is unexpected based on Milky Way disk abundances (e.g., Edvardsson et al. 1993). Perhaps less radical minor merger(s) or accretion(s) also provide a route to forming star clusters under the proviso that sufficient gas is available. The mass of the satellite, its density profile and orbital parameters would determine the degree of heating of any disk present, but would not necessarily lead to its disruption (Huang & Carlberg 1997; Velázquez & White 1999).

We can derive an approximate upper limit on the neutral gas mass of the infalling satellite from the total luminosity of the six IAGCs ( $\sim 6 \times 10^5 L_\odot$ ). Assuming a mass-to-light ratio of 1 for the IAGCs (BC03), and a formation efficiency (i.e.,  $M_{GC}/M_{gas}$ ) of 0.25% (McLaughlin 1999), we obtain  $\sim 2.4 \times 10^8 M_\odot$  of gas required. Extrapolating the amount of gas necessary to form the

estimated  $84 \pm 12$  IAGCs yields a required H I mass of  $\sim 3.4 \times 10^9 M_{\odot}$ . By comparison, the total H I mass of the SMC is  $4.2 \times 10^8 M_{\odot}$  (Stanimirovic et al. 1999), and that of the LMC is  $5 \times 10^8 M_{\odot}$  (Kim et al. 1998). The very similar ages and metallicities of the IAGCs suggests that these objects formed at a similar epoch, and from gas of a similar metallicity. This in itself argues for a single progenitor, and for the clusters to be formed during the hypothetical progenitor’s infall onto M31. For example, the accretion of an SMC-type satellite, and the subsequent accretion of a pre-formed SMC-like cluster system, would yield an age-metallicity relation inconsistent with that which we observe (e.g., Da Costa & Hatzimiditrou 1998; Harris & Zaritsky 2004).

It is difficult to try and associate (spatially or kinematically) the IAGCs with the observed substructure in M31 without having detailed knowledge of the orbit of the satellite giving rise to particular the substructure in question. However, here we speculate briefly. The preliminary orbit of the progenitor of the ‘Andromeda Stream’ (Ibata et al. 2001) appears to be surprisingly radial (and perhaps nearly co-planar) and passes close to the center of M31’s bulge (Ferguson et al. 2002; Ibata et al. 2004). This is consistent with the location of three of the IAGCs. The orbit to the North of the M31 bulge is less well constrained, but would have difficulty passing through the location of all the non-bulge IAGCs (c.f. Figure 17). Kinematically, the Andromeda Stream is at much lower velocities than five of the six IAGCs (the mean velocity of the stream is  $\sim -400 \text{ kms}^{-1}$ ; Ibata et al. 2004), making a direct connection look unlikely.

Ferguson et al. (2002) discuss the possibility that this stream may be associated with M32. Could the IAGCs be associated with M32? There is evidence that M32 has lost a large fraction of its mass (Faber 1973), and has undergone tidal interactions (e.g., Choi et al. 2002). M32 is observed to have no GCs, although its luminosity would predict  $\sim 15$ . These have possibly been stripped by the tidal field of M31 (van den Bergh 2000). It has also been suggested that M32 once possessed significant quantities of gas, and is possibly the remnants of a ‘threshed’ low-luminosity spiral (Bekki et al. 2001; but see also Graham 2002). This suggestion is intriguing since such a spiral may be expected to have a relatively large reservoir of low-metallicity gas. Based upon its integrated spectrum, M32 also has a central mean age similar to the IAGCs, and shows similar low CN values. However it is also significantly more metal-rich ( $[Z/H] \sim 0$ ) than the IAGCs, but this may simply reflect an extended period of star formation in this galaxy (e.g., Schiavon et al. 2004).

Another candidate for the progenitor of the IAGCs is the dwarf elliptical NGC 205. In terms of its light-weighted age and metallicity, this galaxy is very similar to the mean properties of the IAGCs (Mould, Kristian & Da Costa 1984; Lee et al. 1996; Section 4.2). Similar to the case for M32 and the IAGCs, but unlike the bulge of M31, this galaxy exhibits low CN values. It also shows signs of recent star formation (Lee 1996), and the report of an arc-like overdensity spatially coincident with NGC 205 suggests that this satellite is undergoing some tidal disruption (McConnachie et al. 2004). However, without a knowledge of the orbit of this galaxy we refrain from speculating further on its possible connection to the IAGCs.

In summary, we find that the Andromeda spiral appears to have at least four sub-populations of star clusters: one metal-poor and old, one metal-rich and old, one intermediate age and of intermediate-metallicity, and one very young with solar metallicity (Paper I). These younger populations appear kinematically distinct from their older counterparts. A complete spectroscopic survey is necessary to help understand why the globular cluster system of M31 differs so much from our own Galaxy.

## 7. Acknowledgments

We thank Michael Gregg for supplying his Galactic GC spectra in digital form, Javier Cenarro and Kenji Bekki for useful discussions. This research has made use of the SIMBAD database, operated at CDS, Strasbourg, France. This research draws upon data provided by [Dr P. Massey] as distributed by the NOAO Science Archive. NOAO is operated by the Association of Universities for Research in Astronomy (AURA), Inc. under a cooperative agreement with the National Science Foundation. Funding support comes from NSF grant AST 0206139. The data presented herein were obtained at the W.M. Keck Observatory, which is operated as a scientific partnership among the California Institute of Technology, the University of California and the National Aeronautics and Space Administration. The Observatory was made possible by the generous financial support of the W.M. Keck Foundation. This research has made use of the NASA/IPAC Extragalactic Database (NED), which is operated by the Jet Propulsion Laboratory, Caltech, under contract with the National Aeronautics and Space Administration.

## REFERENCES

- Barbuy, B. 1994, *ApJ*, 430, 218
- Barmby, P. & Huchra, J. P. 2000, *ApJ*, 531, L29
- Barmby, P., Huchra, J. P., Brodie, J. P., Forbes, D. A., Schroder, L. L., & Grillmair, C. J. 2000, *AJ*, 119, 727
- Battistini, P. L., Bonoli, F., Casavecchia, M., Ciotti, L., Federici, L., & Fusi-Pecchi, F. 1993, *A&A*, 272, 77
- Battistini, P., Bonoli, F., Braccesi, A., Federici, L., Fusi Pecchi, F., Marano, B., & Borngen, F. 1987, *A&AS*, 67, 447
- Beasley, M.A., Brodie, J.P., Strader, J., Forbes, D.A., Proctor, R.N., Barmby, P. & Huchra, J.P. 2004, *AJ*, (Paper I)
- Beasley, M. A., Hoyle, F., & Sharples, R. M. 2002, *MNRAS*, 336, 168
- Beasley, M. A., Baugh, C. M., Forbes, D. A., Sharples, R. M., & Frenk, C. S. 2002, *MNRAS*, 333, 383

- Bekki, K., Forbes, D. A., Beasley, M. A., & Couch, W. J. 2002, MNRAS, 335, 1176
- Bekki, K., Couch, W. J., Drinkwater, M. J., & Gregg, M. D. 2001, ApJ, 557, L39
- Bellazzini, M., Ibata, R., Ferraro, F. R., & Testa, V. 2003, A&A, 405, 577
- Bonifacio, P., Hill, V., Molaro, P., Pasquini, L., Di Marcantonio, P., & Santin, P. 2000, A&A, 359, 663
- Borges, A. C., Idiart, T. P., de Freitas Pacheco, J. A., & Thevenin, F. 1995, AJ, 110, 2408
- Bica, E., Claria, J. J., & Dottori, H. 1992, AJ, 103, 1859
- Bica, E., Claria, J. J., Dottori, H., Santos, J. F. C., & Piatti, A. E. 1996, ApJS, 102, 57
- Bica, E., Alloin, D., & Schmidt, A. A. 1990, A&A, 228, 23
- Brodie, J. P. & Huchra, J. P. 1991, ApJ, 379, 157
- Brown, T. M., Ferguson, H. C., Smith, E., Kimble, R. A., Sweigart, A. V., Renzini, A., Rich, R. M., & Vandenberg, D. A. 2004, ApJ, 613, L125
- Brown, T. M., Ferguson, H. C., Smith, E., Kimble, R. A., Sweigart, A. V., Renzini, A., Rich, R. M., & Vandenberg, D. A. 2003, ApJ, 592, L17
- Brown, J. A., Wallerstein, G., & Zucker, D. 1997, AJ, 114, 180
- Bruzual, G. & Charlot, S. 2003, MNRAS, 344, 1000 (BC03)
- Buonanno, R., Corsi, C. E., Pecci, F. F., Richer, H. B., & Fahlman, G. G. 1993, AJ, 105, 184
- Buonanno, R., Buscema, G., Fusi Pecci, F., Richer, H. B., & Fahlman, G. G. 1990, AJ, 100, 1811
- Burstein, D., et al. 2004, ApJ, 614, 158
- Burstein, D., Faber, S. M., Gaskell, C. M., & Krumm, N. 1984, ApJ, 287, 586
- Carney, B. W. 1996, PASP, 108, 900
- Choi, P. I., Guhathakurta, P., & Johnston, K. V. 2002, AJ, 124, 310
- Cohen, J. G. 2004, AJ, 127, 1545
- Cohen, J. G., Blakeslee, J. P., & Ryzhov, A. 1998, ApJ, 496, 808 (CBR98)
- Da Costa, G. S. & Hatzidimitriou, D. 1998, AJ, 115, 1934
- Da Costa, G. S., Armandroff, T. E., & Norris, J. E. 1992, AJ, 104, 154
- de Freitas Pacheco, J. A. 1997, A&A, 319, 394
- Demers, S., Battinelli, P., & Letarte, B. 2003, AJ, 125, 3037
- Edvardsson, B., Andersen, J., Gustafsson, B., Lambert, D. L., Nissen, P. E., & Tomkin, J. 1993, A&A, 275, 101
- Faber, S. M. 1973, ApJ, 179, 423
- Ferguson, A. M. N., Irwin, M. J., Ibata, R. A., Lewis, G. F., & Tanvir, N. R. 2002, AJ, 124, 1452

- Fusi Pecci, F., et al. 1996, *AJ*, 112, 1461
- Galleti, S., Federici, L., Bellazzini, M., Fusi Pecci, F., & Macrina, S. 2004, *A&A*, 416, 917
- Graham, A. W. 2002, *ApJ*, 568, L13
- Gratton, R., Sneden, C., Carretta, E., 2004, *ARA&A*, 42, 385
- Gratton, R. G. & Ortolani, S. 1988, *A&AS*, 73, 137
- Gregg, M. D. 1994, *AJ*, 108, 2164
- Harris, J. & Zaritsky, D. 2004, *AJ*, 127, 1531
- Holland, S. 1998, *AJ*, 115, 1916
- Huang, S. & Carlberg, R. G. 1997, *ApJ*, 480, 503
- Hubble, E. 1932, *ApJ*, 76, 44
- Huchra, J. P., Brodie, J. P., & Kent, S. M. 1991, *ApJ*, 370, 495
- Ibata, R., Chapman, S., Ferguson, A. M. N., Irwin, M., Lewis, G., & McConnachie, A. 2004, *MNRAS*, 351, 117
- Ibata, R., Irwin, M., Lewis, G., Ferguson, A. M. N., & Tanvir, N. 2001, *Nature*, 412, 49
- Irwin, M. 1999, "The stellar content of Local Group galaxies", *IAU Symposium*, 192, 409
- Jablonka, P., Bica, E., Bonatto, C., Bridges, T. J., Langlois, M., & Carter, D. 1998, *A&A*, 335, 867
- Jablonka, P., Alloin, D., & Bica, E. 1992, *A&A*, 260, 97
- Jiang, L., Ma, J., Zhou, X., Chen, J., Wu, H., & Jiang, Z. 2003, *AJ*, 125, 727
- Johnson, J. A., Bolte, M., Stetson, P. B., Hesser, J. E., & Somerville, R. S. 1999, *ApJ*, 527, 199
- Kim, S., Staveley-Smith, L., Dopita, M. A., Freeman, K. C., Sault, R. J., Kesteven, M. J., & McConnell, D. 1998, *ApJ*, 503, 674
- Kuntschner, H., Ziegler, B. L., Sharples, R. M., Worthey, G., & Fricke, K. J. 2002, *A&A*, 395, 761
- Larsen, S. S., Brodie, J. P., Sarajedini, A., & Huchra, J. P. 2002, *AJ*, 124, 2615
- Le Borgne, J.-F., et al. 2003, *A&A*, 402, 433
- Lee, H., Yoon, S., & Lee, Y. 2000, *AJ*, 120, 998
- Lee, M. G. 1996, *AJ*, 112, 1438
- Lee, Y., Demarque, P., & Zinn, R. 1994, *ApJ*, 423, 248
- Li, Y. & Burstein, D. 2003, *ApJ*, 598, L103
- Maoz, D., Barth, A. J., Ho, L. C., Sternberg, A., & Filippenko, A. V. 2001, *AJ*, 121, 3048
- Maraston, C. & Thomas, D. 2000, *ApJ*, 541, 126
- Maraston, C. 1998, *MNRAS*, 300, 872
- Martínez-Delgado, D., Zinn, R., Carrera, R., & Gallart, C. 2002, *ApJ*, 573, L19

- McConnachie, A. W., Irwin, M. J., Lewis, G. F., Ibata, R. A., Chapman, S. C., Ferguson, A. M. N., & Tanvir, N. R. 2004, MNRAS, 351, L94
- McLaughlin, D. E. 1999, AJ, 117, 2398
- McWilliam, A. & Rich, R. M. 1994, ApJS, 91, 749
- Milone, A., Barbuy, B., & Schiavon, R. P. 2000, AJ, 120, 131
- Morrison, H. L., Harding, P., Perrett, K., & Hurley-Keller, D. 2004, ApJ, 603, 87
- Mould, J., Kristian, J., & Da Costa, G. S. 1984, ApJ, 278, 575
- Perrett, K. M., Bridges, T. J., Hanes, D. A., Irwin, M. J., Brodie, J. P., Carter, D., Huchra, J. P., & Watson, F. G. 2002, AJ, 123, 2490
- Persson, S. E., Aaronson, M., Cohen, J. G., Frogel, J. A., & Matthews, K. 1983, ApJ, 266, 105
- Peterson, R. C., Carney, B. W., Dorman, B., Green, E. M., Landsman, W., Liebert, J., O’Connell, R. W., & Rood, R. T. 2003, ApJ, 588, 299
- Ponder, J. M., et al. 1998, AJ, 116, 2297
- Proctor, R.N., Forbes, D.A., Beasley, M.A., 2004 (astro-ph/0409526) (PFB04)
- Proctor, R. N., Forbes, D. A., Hau, G. K. T., Beasley, M. A., De Silva, G. M., Contreras, R., & Terlevich, A. I. 2004, MNRAS, 349, 1381
- Proctor, R. N. & Sansom, A. E. 2002, MNRAS, 333, 517
- Puzia, T. H. 2003, Ph.D. Thesis, Sternwarte Muenchen Scheinerstr.
- Puzia, T. H., Saglia, R. P., Kissler-Patig, M., Maraston, C., Greggio, L., Renzini, A., & Ortolani, S. 2002, A&A, 395, 45 (P02)
- Rabin, D. M. 1981, Ph.D. Thesis, California Inst. of Tech., Pasadena.
- Rich, R. M., et al. 1997, ApJ, 484, L25
- Rich, R. M., Mighell, K. J., Freedman, W. L., & Neill, J. D. 1996, AJ, 111, 768
- Robin, A. C., Reylé, C., Derrière, S., & Picaud, S. 2003, A&A, 409, 523
- Rose, J. A. 1985, AJ, 90, 1927
- Rose, J. A. 1984, AJ, 89, 1238
- Rosenberg, A., Saviane, I., Piotto, G., & Held, E. V. 1998, A&A, 339, 61
- Sargent, W. L. W., Kowal, C. T., Hartwick, F. D. A., & van den Bergh, S. 1977, AJ, 82, 947
- Schiavon, R. P., Caldwell, N., & Rose, J. A. 2004a, AJ, 127, 1513
- Schiavon, R. P., Rose, J. A., Courteau, S., & MacArthur, L. A. 2004b, ApJ, 608, L33
- Schiavon, R. P., Faber, S. M., Castilho, B. V., & Rose, J. A. 2002, ApJ, 580, 850
- Smecker-Hane, T.A., McWilliam, A., 2003 (astro-ph/0205411)
- Spinrad, H. & Schweizer, F. 1972, ApJ, 171, 403

- Stanek, K. Z. & Garnavich, P. M. 1998, *ApJ*, 503, L131
- Stanimirovic, S., Staveley-Smith, L., Dickey, J. M., Sault, R. J., & Snowden, S. L. 1999, *MNRAS*, 302, 417
- Stephens, A. W., et al. 2001, *AJ*, 121, 2584
- Stetson, P. B., Hesser, J. E., Smith, G. H., Vandenberg, D. A., & Bolte, M. 1989, *AJ*, 97, 1360
- Strader, J., Brodie, J. P., & Forbes, D. A. 2004, *AJ*, 127, 295
- Tantalo, R., Chiosi, C., Munari, U., Piovan, L. & Sordo, R. 2004, (astro-ph/0406314)
- Tegmark, M., et al. 2004, *Phys. Rev. D.*, 69, 103501
- Terlevich, A. I. & Forbes, D. A. 2002, *MNRAS*, 330, 547
- Thomas, D., Maraston, C., & Korn, A. 2004, *MNRAS*, 351, L19
- Thomas, D., Maraston, C., & Bender, R. 2003, *MNRAS*, 339, 897 (TMB03)
- Trager, S. C. 2004, *Origin and Evolution of the Elements*, Carnegie Observatories Centennial Symposia, Eds. A McWilliam and M. Rauch, p.391
- Trager, S. C., Faber, S. M., Worthey, G., & González, J. J. 2000, *AJ*, 119, 1645
- Trager, S. C., Worthey, G., Faber, S. M., Burstein, D., & Gonzalez, J. J. 1998, *ApJS*, 116, 1
- Tripicco, M. J. & Bell, R. A. 1995, *AJ*, 110, 3035
- Tripicco, M. J. & Bell, R. A. 1992, *AJ*, 103, 1285
- Tripicco, M. J. 1989, *AJ*, 97, 735
- van den Bergh, S. 2000, in *The galaxies of the Local Group*, by Sidney Van den Bergh. Published by Cambridge, UK: Cambridge University Press, 2000 Cambridge Astrophysics Series, vol no: 35
- van den Bergh, S. 1999, *A&A Rev.*, 9, 273
- van den Bergh, S. 1969, *ApJS*, 19, 145
- Vazdekis, A. 1999, *ApJ*, 513, 224 (V99)
- Vazdekis, A., Peletier, R. F., Beckman, J. E., & Casuso, E. 1997, *ApJS*, 111, 203
- Velazquez, H. & White, S. D. M. 1999, *MNRAS*, 304, 254
- Worthey, G. & Ottaviani, D. L. 1997, *ApJS*, 111, 377
- Worthey, G. 1994, *ApJS*, 95, 107
- Worthey, G., Faber, S. M., Gonzalez, J. J., & Burstein, D. 1994, *ApJS*, 94, 687
- Zinn, R. & West, M. J. 1984, *ApJS*, 55, 45
- Zoccali, M., Renzini, A., Ortolani, S., Bica, E., & Barbuy, B. 2001, *AJ*, 121, 2638

Table 1. Metallicities, Ages, Abundance Ratios and Horizontal Branch Morphologies of the M31 Clusters.

Name	$[Z/H]^a$ (dex)	Age <sup>a</sup> (Gyr)	$[\alpha/Fe]^a$ (dex)	$[Z/H]^b$ (dex)	Age <sup>b</sup> (Gyr)	$[\alpha/Fe]^b$ (dex)	Ca II	HBR <sup>c</sup>	CN Strong?
126-184	-1.38	3.4	0.05	-1.18	5.5	0.40	1.424	-1.00	N
±	0.38	1.0	0.20	0.22	3.5	0.10			
134-190	-0.95	9.1	0.04	-0.72	11.9	0.30	1.320	-1.00	Y
...	0.10	2.2	0.50	0.25	1.9	0.30			
158-213	-0.90	9.9	0.12	-0.75	12.1	0.10	1.109	-0.89	Y
...	0.15	2.7	0.20	0.15	0.9	0.10			
163-217	-0.35	10.6	-0.11	-0.15	10.2	0.10	1.312	-1.00	Y
...	0.25	3.7	0.10	0.20	4.8	0.10			
225-280	-0.25	8.4	0.26	-0.30	9.1	0.10	1.246	-1.00	Y
...	0.10	1.9	0.10	0.15	1.2	0.10			
234-290	-0.85	10.3	0.01	-0.65	11.7	0.20	1.120	-0.95	Y
...	0.15	3.2	0.10	0.17	5.7	0.10			
292-010	-1.35	2.7	0.60	-1.23	5.9	0.50	0.992	-0.21	N
...	0.55	1.2	0.20	0.18	3.4	0.10			
301-022	-1.15	3.2	0.15	-1.08	6.2	0.20	1.501	-1.00	N
...	0.30	1.8	0.10	0.40	1.1	0.40			
304-028	-1.60	12.9	0.15	-1.45	11.9	0.00	0.769	1.00	Y
...	0.45	4.7	0.00	0.43	3.9	0.00			
310-032	-1.75	19.5	-0.05	-1.60	11.4	0.10	0.938	0.10	Y
...	0.35	2.1	0.50	0.43	3.5	0.20			
313-036	-0.85	8.8	0.21	-0.70	11.7	0.20	1.296	-1.00	Y
...	0.35	1.2	0.20	0.33	0.9	0.40			
328-054	-1.80	16.8	0.35	-1.50	13.3	0.50	0.970	-0.08	Y
...	0.35	5.2	0.00	0.30	1.1	0.10			
337-068	-0.80	2.6	0.40	-1.00	6.6	0.20	1.371	-1.00	N
...	0.17	1.9	0.10	0.17	3.2	0.20			
347-154	-2.25	8.7	0.25	-1.93	9.9	0.00	0.734	1.00	Y
...	0.10	5.7	0.20	0.47	4.0	0.20			
350-162	-1.65	9.8	0.35	-1.52	12.4	0.20	0.914	0.24	Y
...	0.40	2.5	0.30	0.17	4.7	0.30			
365-284	-1.45	9.2	0.15	-1.23	10.4	0.20	0.814	0.82	Y
...	0.40	3.1	0.20	0.50	2.2	0.10			
383-318	-0.55	10.3	0.14	-0.40	10.6	0.30	1.709	-1.00	Y
...	0.15	2.2	0.10	0.12	1.3	0.30			
393-330	-1.00	10.0	-0.05	-0.80	11.9	0.00	1.522	-1.00	Y
...	0.45	1.8	0.00	0.38	1.3	0.30			
398-341	-0.50	12.1	0.22	-0.33	14.7	0.20	1.204	-1.00	Y
...	0.30	1.5	0.30	0.28	3.7	0.00			
401-344	-2.25	9.2	0.25	-2.10	15.0	0.30	0.679	1.00	Y
...	0.40	5.8	0.30	0.15	5.1	0.20			
NB16	-0.90	2.0	0.53	-0.95	4.6	0.40	1.232	-1.00	N
...	0.15	1.4	0.10	0.22	0.8	0.10			
NB67	-0.95	2.2	0.54	-0.90	4.7	0.50	1.273	-1.00	N
...	0.15	1.4	0.30	0.10	0.3	0.20			
NB89	-0.55	8.3	0.24	-0.65	10.4	0.20	1.128	-1.00	Y
...	0.10	2.6	0.10	0.12	2.7	0.10			



<sup>a</sup>Bruzual & Charlot (2003) models.

<sup>b</sup>Thomas, Maraston & Bender (2003) models.

<sup>c</sup>ee et al. 1994.